Arabian Journal of Geosciences (2019) 12: 780
https://doi.org/10.1007/s12517-019-4942-7

REVIEW PAPER

Hydrogeochemical characterization and water quality assessment of springs in the Emirdağ (Afyonkarahisar) basin, Turkey

Fatma Aksever[1]

Received: 25 May 2019 / Accepted: 30 October 2019 / Published online: 11 December 2019

Abstract

The investigation area includes the Emirdağ (Afyonkarahisar) basin and its vicinity located in the Upper Sakarya section of Central Anatolia Region. Mesozoic aged recrystallized limestone and dolomites forming the basis of the investigation area, Cretaceous ophiolites, Neogene aged pyroclastic rocks, and unconstructed terrestrial clastics are the dominant rocks. There are many natural water springs in this region. Springs are the primary source for drinking and household needs. Besides, these springs are used for agricultural irrigation, trout plant, etc. In this study, a total of 10 spring samples collected from the Emirdağ basin and waters were evaluated for hydrochemical processes, drinking water chemistry, and irrigation water quality. Generally, the yield of water springs which are discharged from volcanic rocks and limestones varies between 0.02 and 2.00 l/s. The pH, temperatures, electrical conductivity, total dissolved solids, and redox potential are changed between 6.53 and 7.86, 11.50 and 17.80 °C, 251 and 790 µS/cm, 132 and 490 mg/l, and 204.10 and 262.30 mV, respectively. The major ion sequence of waters is generally $Ca^{2+} > Mg^{2+} > Na^{+} > K^{+}$ and $HCO_3^{-} > SO_4^{2-} > Cl^{-} > F^{-} > PO_4^{3-}$. Ca^{2+}, Mg^{2+}, and HCO_3^{-} are the dominant ions in the groundwater of the study area. The hydrochemical facies of the majority of the study area spring samples are "$CaMgHCO_3$" and "$CaMgSO_4$" types. The distribution of sample points in the Gibbs diagram suggests a rock dominance area. The Schoeller drinkability diagram shows very good and good quality waters. The springs' suitability for irrigation classification suggests that more than 90% of the water sampling locations are suitable for irrigation. However, the water quality of Pınarbaşı spring is different from the other springs due to the high electrical conductivity value (790 µS/cm). Also, the Wilcox and US Salinity Laboratory diagrams show that groundwater samples are good for irrigation. As a result of the analysis of nitrogen compounds, nitrate concentration in the Ağzıören (64.09 mg/l) and Ufukpınar (62.01 mg/l) springs only exceeds drinking water standards. It is thought that the increase of nitrate in these springs is due to agricultural pollution. The values in the isotopic composition are above the local and global meteoric water lines, probably indicating similarity in the mechanism of recharge, and the tritium level shows recent groundwater contribution. The springs generally are represented as shallow and have fast circulation.

Keywords Emirdağ (Afyonkarahisar) basin · Water springs · Hydrochemistry · Stable isotopes

Introduction

In recent years, investigations have focused on natural springs because spring waters are a significant resource and springs can have the qualities suitable for all conditions like drinking, usage, irrigation, and industrial purposes in many regions. Therefore, it is much more vital to comprehensively understand the controlling factors of springs' chemistry and its quality. For the past years, a number of researchers have emphasized on the springs' quality characteristics and its impact on water chemistry and its suitability for various purposes. Hydrochemical parameters are important to assess the springs' water quality. The quality of spring waters is influenced by factors such as geogenic and anthropogenic. There are many studies about spring waters in the literature (Ryan and Meiman 1996; Prasad and Bose 2001; Ragno et al. 2007; Michalik 2008; Ako et al. 2012; Shigut et al. 2017). Especially, evaluations of the main geochemical processes and the impact of anthropogenic and natural sources of contamination on groundwater quality of the aquifer system used for domestic and agricultural purposes were investigated in

---

Responsible Editor: Helder I. Chaminé

✉ Fatma Aksever
fatmaaksever@sdu.edu.tr

[1] Department of Geological Engineering, Süleyman Demirel University, Isparta, Turkey

detail by Barbieri et al. (2017, 2019). A spring's discharge characteristics and water quality can be predicted from its geological and hydrogeological settings. The hydrogeochemical characteristics of groundwater reflect the source of the main components, the type of water, its formative mechanism, the water–rock interaction, and the environment of the groundwater reservoir (Sun et al. 2014; Saxena and Ahmed 2001; Taheri et al. 2017). The hydrochemistry of spring waters provides information regarding water–rock interaction along flow paths (Kanduč et al. 2012). Also, springs can provide information about local and regional groundwater hydrology (Larsen et al. 2001). Therefore, geogenic and anthropogenic factors are understood to be the principal cause for the springs' pollution. The physicochemical characteristics of groundwater are also important to determine the effects of natural processes (e.g., the dissolution of minerals, ion exchange, evaporation, and precipitation) and human activities and enable the evaluation of its quality for agricultural irrigation purposes (Jang et al. 2016; Iqbal et al. 2017; Mostaza-Colado et al. 2018; Khalid 2019). The quality of irrigation water can be assessed with various water quality indices that are widely used worldwide. These include salinity hazard (SH), sodium percentage (Na%), sodium adsorption ratio (SAR), residual sodium carbonate (RSC), residual sodium bicarbonate (RSBC), soluble sodium percentage (SSP), magnesium ratio (MR), permeability index (PI), Kelley's ratio (KR), synthetic harmful coefficient (K), and irrigation coefficient (Ka) (Li et al. 2016; Tahmasebi et al. 2018; Verma et al. 2017; Abdulhussein 2018; Khalid 2019, Xu et al. 2019).

The Emirdağ basin has rich water supply. Springs are the major water resource for drinking water and agricultural development of the Emirdağ basin. Therefore, the aims of this study were to investigate the origin of the spring waters and to determine the suitability of spring water for drinking and irrigation, using major ions, hydrochemical processes, and environmental isotopes, various criteria to Emirdağ basin.

Field site descriptions

The investigation area covers Emirdağ district and its vicinity on the border of Central Anatolia and in the northeast of the Aegean Region. The region is lies between 39° 1′ 33.7404″ latitude and 31° 9′ 12.4200″ longitude (Fig. 1). The annual mean precipitation is 421 mm in Emirdağ. The least amount of precipitation occurs in August and the mean in this month is 12 mm. In May, the precipitation reaches its peak, with a mean of 56 mm. The difference in precipitation between the driest month and the wettest month is 44 mm. The annual mean temperature is 11.0 °C in the region. The temperatures are highest on mean in July, at around 21.1 °C. At 0.3 °C on mean, January is the coldest month of the year (https://tr.climate-data.org/asya/tuerkiye/afyonkarahisar/emirdag-21371, Erişim tarihi ve saati: 20 Sept 2019, 14:15). The average elevation of the Emirdağ plain varies between 950 and 1100 m, which is surrounded by Adaçal mountain (1259 m) in the northwest, Karadağ in the west, and Sakardağ and Karaçal crystalline limestone in the south (Ardel 1955). The area of the Emirdağ district is 2000 km^2, which forms a transition zone between the Aegean and Central Anatolian Regions. The Emirdağ plain extending in the direction of NW–SE constitutes the Quaternary aged alluvium, which is the youngest unit of the investigation area. The Emirdağ mountainous mass, which is located to the south of the investigation area, is composed of Mesozoic limestones and volcanic rocks (Canlı 2007). The Triassic crystallized limestones and dolomites, which form the base of the investigation area, are called "Emirdağ limestones" by Wirtz (1955). The geological, mineralogical, geochemical, and physical properties of the Emirdağ limestones have been determined in many studies (Türksoy 2010; Yılmaz et al. 2011; Yıldız et al. 2014).

The inadequate amount of groundwater and increasing of groundwater depth gradually reduced the population in rural areas of Emirdağ Province (Yakar 2009). The people of Emirdağ district generally migrated abroad. However, the majority of the people come to Emirdağ in summer and increase the population of the district. Therefore, the demand for agricultural and domestic water use in the province is increasing in summer. Springs in the region discharged from high elevations are mainly used for drinking, irrigation, and domestic use. In this study, the hydrogeochemical properties of springs have been examined. The results of research are of great importance for the first time in the region.

Materials and methods

The 1/100,000 scale geology map covering Emirdağ district and its vicinity has been revised in the direction of literature studies within the scope of the study. The lithological units in the investigation area are classified according to their aquifer potential and are shown on the geological map. Water samples were collected from 10 springs in wet seasons, 2018. Samples were taken in 100 ml sterile polyethylene bottles with plastic sealing cap, and high purity HCl (hydrochloric acid) was added and acidified to pH < 2 (for cation analysis). Sampling site geopositions were determined using a Magellan Explorist 710 handheld GPS and sample locations were processed on the geological map. The various physicochemical parameters such as pH, redox potential (Eh), discharge temperature (*T*), electrical conductivity (EC), and total dissolved solids (TDS) were measured in situ using potable HACH HQ40D handheld device after calibration.

The groundwater samples were analyzed for various hydrochemical parameters, such as calcium (Ca^{2+}), magnesium (Mg^{2+}), sodium (Na^+), potassium (K^+), chloride (Cl^-), sulfate (SO_4^{2-}), bicarbonate (HCO_3^{2-}), fluoride (F^-),

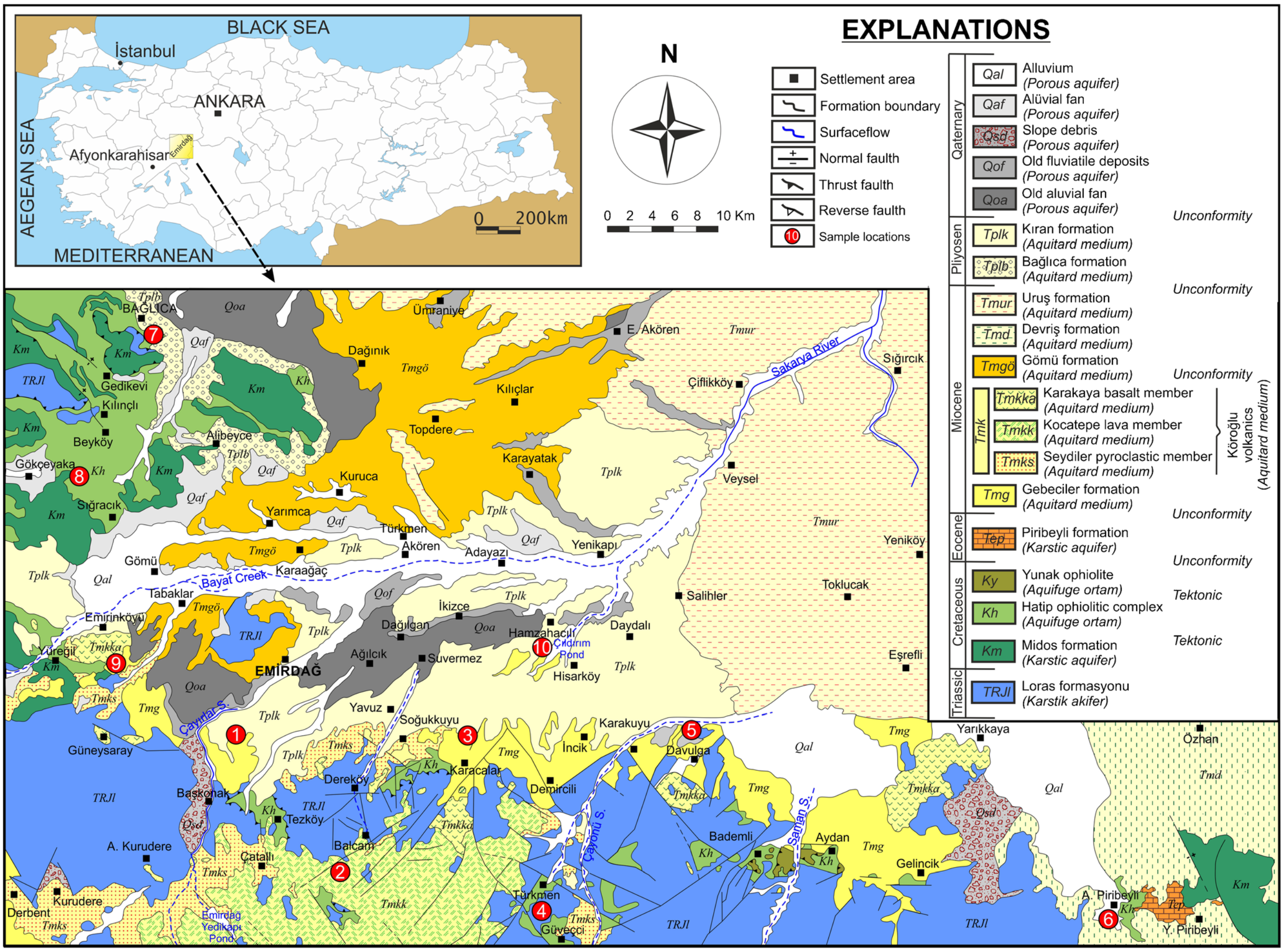

Fig. 1 Geological and hydrogeological map of the study area (revised from Umut 2008; Acarlar et al. 2009; Öcal et al. 2011)

phosphate (PO_4^{3-}), and nitrogen derivatives including nitrate (NO_3^-), nitrite (NO_2^-), and ammonium (NH_4^+) ions, and the analyses were carried out at the Hacettepe University Water Chemistry and Environmental Tritium Laboratories. The chemical composition was determined using standard analytical methods (The American Public Health Association (APHA), The American Water Works Association (AWWA), and The Water Pollution Control Federation (WPCF)) with the Standard Methods (APHA and WEF 2012) for the Examination of Water and Waste Water test. Trace elements (Al, As, B, Ba, Br, Cd, Cr, Cu, Fe, Hg, Mn, Ni, Pb, U, Sb, Se, and Zn) were determined using the inductively coupled plasma-mass spectrometer (ICP-MS) instrument at Canada Bureau Veritas Mineral Laboratories (Acme Analytical Laboratories). All of these results were evaluated in detail and compared with the water quality guidelines of WHO (2011) and TS-266 (2005).

Relations between physical–chemical parameters and concentrations of elements were determined by Spearman's correlation coefficient using the statistical software SPSS 15.0 (Statistical Package for the Social Sciences). For identification, the chemical data of spring samples were plotted and interpreted using Piper, Gibbs, Schoeller, Schoeller drinkable, US Salinity Laboratory, and Wilcox diagrams. Interpretation of the results of the hydrochemical analysis was made with AquaChem software.

Stable isotope techniques were used to interpret recharge mechanisms of the aquifer in the investigation area. Stable isotope samples were taken in 1-l sterile polyethylene bottles. Analyses for stable isotopes oxygen-18 ($\delta^{18}O$), deuterium (δ^2H), and radioactive isotopes of hydrogen (tritium-δ^3H) in water samples were carried out at the Ankara Technical Research and Quality Control Department of Isotope Laboratory and Director in the State Hydraulic Works (SHW). $\delta^{18}O$ and δ^2H from isotopic compositions of the samples were determined using the International Atomic Energy Agency IAEA-Equilibration method. Also, δ^3H was determined using the IAEA-liquid siltation counting (LSC) technique. The isotope results are expressed with respect to the global meteoric water line (GMWL). The analytical errors were ± 0.1 and ± 1%, respectively. Tritium concentration was identified using tritium unit (TU). The tritium units are

1 TU = 0.1183 Bq/l. The precision of measurements is ± 1 TU. Measurement uncertainty in experimental results is calculated at 95% CI (confidence interval; K = 2). The isotopic compositions of waters within the investigation area were compared with the GMWL and Ankara meteoric water line (AMWL).

Results and discussion

Geological setting

In the investigation area, the Kütahya Bolkardağı Belt rocks and ophiolites belonging to the Bozkır Union cover rocks are located (Fig. 1). The basement of the investigation area is the Mesozoic aged Loras formation consisting of limestone and dolomites belonging to KütahyaBolkardağı Belt. The formation basin begins with Middle-Upper Triassic aged dolomite and recrystallized limestones. The unit is continuing upwards with Middle Triassic–Upper Jurassic aged, oolitic, algal limestones and dolomites. The formation is ending with Jura-Cretaceous aged recrystallized limestone and cherty recrystallized limestones. Loras formation is transitional with Midos formation which is composed of Upper Cretaceous aged pelagic sediments. The formation consists of micritic limestone, clayey limestone, mudstone, chert, and shale.

The Yunak ophiolite and Hatip ophiolitic rocks belonging to the Bozkır Unit tectonically overlie the underlying Mesozoic units. Upper Cretaceous aged Hatipophiolitic rock consists of rocks containing neritic–pelagic limestone, marl, sandstone–shale alternation, conglomerate, sericite–chlorite schist, phyllite, volcanite, and ultramafic blocks. The Upper Cretaceous Yunakophiolite, consisting of mafic and ultramafic rocks such as serpentinized peridotite, gabbro, and diabase, settled as a nap on the region. It is tectonically contacted with the Hatipophiolite complex.

The Lower Eocene aged Piribeyli formation consisting of clayey limestone, cherty nodule, and nummulitic–micritic limestones overlies ophiolitic rocks unconformably. The Middle Miocene aged Gebeciler formation overlies on all the lower units unconformably. The formation begins with basal conglomerate, pebbly sandstone, marl, clayey limestone, and limestone, followed by tuff-tuffite–marl, clayey limestone, and limestone.

The Seydiler pyroclastic member of Köroğlu volcanics of Middle Miocene ages is laterally and vertically transitional with the Gebeciler formation. Pyroclastics of the Seydiler pyroclastic member consist of shale, back-fall deposits, ignimbrite, and block-ash flows. The lavas forming the Köroğlu volcanics are defined as two members. One of them is the Karakaya basalt member composed of basalt and trachybasalt, and the other, Kocatepe lava member consisting of trachyte and trachyandesite containing large crystals and abundant biotite crystals.

Upper Miocene aged Gömü formation, consisting of rugged rocks such as sandstones, claystones, and conglomerates, unconformably overlies the volcanics. Upper Miocene aged, Devriş formation consisting of marl, limestone, and claystones and the Uruş formation composed of limestone, marl, gypsum, sandstone, claystone, and conglomerate are transitional with Gömü formation. The Pliocene aged Bağlıca formation, consisting of conglomerate, sandstone, and claystone, unconformably overlying Upper Miocene aged units, is transitional with Kıran formation. The Kıran formation, where the dominant lithology is formed by pebbles, includes rugged rocks such as sandstone, claystone, siltstone, and clayey limestone. The age range of the unit extends from the Pliocene to the Lower Pleistocene.

Quaternary units formed by materials such as loose gravel, clay, sand, and mud are distinguished in the investigation area as old alluvial fan, old fluviatile deposits, slope debris, alluvial fan, and alluvium (Özcan et al. 1990; Umut 2008; Acarlar et al. 2009; Öcal et al. 2011).

Hydrogeological setting

The lithological units in the investigation area are classified according to their hydrogeological properties. Alluvium is consisting of loose clay, silt, sand, gravel, block-sized materials, and alternating combinations of these. Alluvium has a wide spread in the plain which can be taken with significant amounts of water from gravel and sand levels. Old alluvial fan, old fluviatile deposits, slope debris, and alluvial fan are intertwined with alluvium, which covered large areas in the northern and southern parts of the plain, formed as “porous aquifer” in the investigation area. Drinking and usage water in the towns and villages are provided from drilling wells opened in alluvium and springs.

The calcareous rocks (clayey limestone, nummulitic–micritic limestones, limestone, and dolomite levels within Piribeyli, Midos, and Loras formations) in the investigation area have a permeable feature. The limestones, which are melt-fractured, are “karstic aquifers.”

Gebeciler formation, Köroğlu volcanics, and members are Neogene aged volcanic rocks. These rocks have wide spreading in the investigation area and are semipermeable. Volcanosedimanter units are composed of tuff, tuffite, andesite, basalt, trachyte, ignimbrite, etc., and lithologists do not allow movement of groundwater because their pores are too low. However, secondary porosity in the fractured and cracked part of the unit is increased and groundwater movement occurs. The Gömü, Devriş, Uruş, Kıran, and Bağlı formations become permeable with medium-thick bedded sandstone, limestone levels, and loose sand or carbonate cemented conglomerates. These units, which have semipermeable characteristics, symbolize the “aquitard medium” in the investigation area because of they contain impermeable levels such as marl, claystone, siltstone, and mudstone. Groundwater is taken from the sandstone and conglomerate levels of the Neogene units. Groundwater level is 59.5 m in Dağınık village on Gömü formation. Groundwater levels in the wells on the Uruş formation are 46.3 m (Toklucak village) and 28.7 m (Yarıkkaya village) (Canlı 2007).

Hatip ophiolitic complex consisting of neritic–pelagic limestone, marl, sandstone–shale, conglomerate, sericite–chlorite schist, phyllite, volcanite, and ultramafic blocks. The neritic–pelagic limestone, conglomerate, and sandstone levels may contain groundwater in the fracture and crack region. But the sericite–chlorite schist and phyllite levels have impermeable characteristic. The complex contacted with limestones in the northwest and south regions and spring discharges are observed in these regions of the investigation area. So, Hatip ophiolitic complex is interpreted as a low permeability medium. Yunak ophiolite which is composed of the serpentinized peridotite, gabbro, and dunite mafic and ultramafic rocks is impermeable. Another impermeable unit is due to the marls and schists it contains, and the unit is hydrogeologically impermeable and represents the "aquifuge medium" (Fig. 1).

Hydrology

The most important surface in the investigation area is Sakarya River. Also, the river is Turkey's third longest and largest river in northwestern Anatolia. The length of the river is 824 km and the width of the feeding basin is 53.800 km^2. The river is born as Bayat creek from the Bayat plateau in the northern part of Afyonkarahisar. The highest water level in the river, which has an irregular regime, is observed in the spring season (TMMOB 2012). The wetland areas of the Sakarya River, which has large water transport capacity, are entered into force as "National Wetland Area" in 2009 by the General Directorate of Nature Conservation and National Parks of the Turkish Republic Ministry of Forestry and Water Affairs (Meriç and Çağırankaya 2013).

There are many seasonal streams (Çayırlar, Çayönü, Saman) along the Sakarya River in the investigation area. There are two small dams within the investigation area. The Emirdağ Yedikapı dam was constructed on the Yedikapı River with 2.58 hm^3 of water storage capacity. This dam is used for the drinking water requirement of Emirdağ Province (DSİ 2018). The Çıldırım dam is located in Hamzahacılı village and constructed for irrigation.

Springs Springs are recharged from volcanics and limestones in the investigation area. These springs are discharged from high elevations and used for drinking water, irrigation, domestic purposes. The springs are generally in the form of strata, karstic, fault, and crack springs. The springs that are located in the north and south of the investigation area are as follows Emirdağ, Tezköy, Emirdede, Elmalı, Ağzıören, Aşağıpiribeyli, Karadağ, Uykucupınar, Ufukpınar, and Pınarbaşı springs. The yields and discharged temperatures of the springs are in the range of 0.02–2.00 l/s and 11.50–17.80 °C, respectively.

Hydrochemistry

A total of 10 different water samples were collected to determine the hydrogeochemical and quality properties of the springs in the investigation area. Water samples were analyzed for multiple chemical constituents' major ions, nitrogens, trace elements, and stable isotopes. The samples taken from the springs were found in Emirdağ (1), Tezköy (2), Emirdede (3), Elmalı (4), Ağzıören (5), Aşağıpiribeyli (6), Karadağ (7), Uykucupınar (8), Ufukpınar (9), and Pınarbaşı (10).

Physicochemical parameters

Physicochemical parameters such as hydrogen ion concentration (pH), discharge temperature (T, °C), EC (µS/cm), TDS (mg/l), dissolved oxygen (DO, mg/l), and redox potential (Eh) are measured in situ. pH is one of the most important parameters in water chemistry. The pH values of the samples were between 6.53 and 7.86 and all pH values are within the permissible limits ($6.5 \leq \text{pH} \geq 9.5$) of WHO (2011) and TS-266 (2005) for drinking water. The water samples are "basic character" waters in the study area. The temperature and EC values of these springs are between 11.50 and 17.80 °C and between 251 and 790 µS/cm. The maximum permissible limit of electrical conductivity as per TS-266 (2005) is 650–2500 µS/cm. The total dissolved solid values were between 132 and 490 mg/l and within the permissible level of TDS for drinking water of 600–1000 mg/l^{-1} for WHO (2011). The redox potential and salinity values measured 204.10–262.30 mV and 0.03–0.2‰, respectively. The hardness of the springs is determined as 4.00–53.47 Fr (Table 1).

Hydrogeochemical facies

According to the chemical analysis results, the major cation and anion sequence of spring waters is $Ca^{2+} > Mg^{2+} > Na^+ > K^+$ and $HCO_3^- > SO_4^{2-} > Cl^- > F > PO_4^{3-}$. The dominant ions are Ca^{2+}, Mg^{2+}, and HCO_3^- due to water–rock interaction. Limestones units (Loras, Midos, and Piribeyli formations) are dominant in the investigation area. These springs are interacting with limestones. The chemical analysis values of spring waters are in compliance with the drinking water standard.

Fluoride concentration values of the spring waters range from 0.02 to 1.49 mg/l. Fluoride mainly occurs in groundwater as a natural constituent. The Ağzıören spring sample showed fluoride concentration (1.49 mg/l) exceeding the WHO (2011) guideline limit (1.5 mg/l) for drinking water.

Table 1 Results of analysis of springs in the study area

Physical parameters													
Sample ID		E-1	E-2	E-3	E-4	E-5	E-6	E-7	E-8	E-9	E-10	Drinking Water Standards	
Sampling location		Emirdağ	Tezköy	Karacalar	Türkmen	Davulga	Aşağıpiribeyli	Bağcılar	Beyköy	Köseli	Hamzahacılı	TS-266 (2005)	WHO (2011)
Spring		Emirdağ	Tezköy	Emirdede	Elmalı	Ağzıören	Aşağıpiribeyli	Karadağ	Uykucupınar	Ufukpınar	Pınarbaşı		
Sampling date		29 January 2018	29 January 2018	29 January 2018	29 January 2018	29 January 2018	29 January 2018	30 January 2018	30 January 2018	30 January 2018	30 January 2018		
Location (UTM)	*X* (E)	340068	340637	347971	352084	358704	378848	333395	332048	332404	355219		
	Y (N)	4320115	4311417	4315942	4308110	4317888	4309072	4336987	4332487	4320259	4323223		
Altitude	*Z* (m)	983	1434	1018	1245	1002	973	1084	1084	1010	877		
Discharge	l/s	0.02	0.60	0.04	0.05	0.06	0.70	0.55	0.28	0.04	2.00		
Temperature (*T*)	°C	13.1	12.7	11.5	13.3	12.2	12.9	12	12.2	11.6	17.8		
Electrical conductivity (EC)	µS/cm	251	690	500	340	410	510	470	580	240	790	650–2500	
pH		6.53	7.35	7.38	7.61	7.55	7.3	7.86	7.05	7.83	7.01	6.5–9.5	6.5–8.5
Total dissolved solids (TDS)	mg/l	132	340	240	150	200	260	230	290	490	400		600–1000
Redox potential (Eh)	mV	249.5	261.1	260.6	262.3	252.4	253.3	218	226.7	211.6	204.1		
Salinity	‰	0.09	0.07	0.04	0.06	0.2	0.03	0.2	0.17	0.19	0.46		
Total hardness (TH)	°F	5.38	6.25	4.00	6.99	21.10	33.14	26.59	40.22	21.11	53.47		
Chemical parameters													
Na^+	mg/l	6.84	5.17	3.54	4.29	12.70	8.24	3.14	11.43	8.26	37.22	200	200
K^+	mg/l	2.71	2.26	1.30	0.84	1.58	1.97	0.28	2.98	0.97	3.95		3000
Mg^{2+}	mg/l	4.89	5.31	2.80	4.35	10.36	7.27	3.05	7.82	6.20	41.78		
Ca^{2+}	mg/l	13.50	16.23	11.43	20.84	67.47	120.83	101.56	148.32	74.38	145.43		
Cl^-	mg/l	1.38	0.86	1.69	1.47	8.01	8.51	1.92	7.00	8.90	24.81	250	250
SO_4^{2-}	mg/l	55.28	27.16	2.89	4.32	11.97	12.79	9.47	23.80	15.41	152.23	250	500
HCO_3^{2-}	mg/l	18.30	54.90	36.60	91.50	201.30	347.70	292.80	420.90	183.00	488.00		
F^-	mg/l	0.28	0.21	0.03	0.06	1.49	0.27	0.02	0.12	0.14	0.33	1.5	1.5
PO_4^{3-}	mg/l	0.00	0.09	0.15	0.22	0.19	0.09	0.00	0.00	0.00	0.00		
Water type		$CaMgSO_4$	$CaMgHCO_3$	$CaMgHCO_3$	$CaMgHCO_3$	$CaMgHCO_3$	$CaMgHCO_3$	$CaMgHCO_3$	$CaMgHCO_3$	$CaMgHCO_3$	$CaMgHCO_3$		
Hydrochemical ratio													
Ca^{2+}/Mg^{2+}	meq/l	1.67	1.85	2.47	2.90	3.95	10.08	20.21	11.51	7.28	2,11		
Na^+/K^+	meq/l	4.29	3.88	4.63	8.67	13.67	7.10	19.20	6.53	14.43	16.01		
CAI-I	meq/l	− 8.44	− 10.69	− 2.93	− 4.01	− 1.62	− 0.70	− 1.65	− 1.91	− 0.53	− 1.46		
CAI-II	meq/l	− 0.22	− 0.16	− 0.16	− 0.10	− 0.08	− 0.03	− 0.02	− 0.05	− 0.03	− 0.09		
Nitrogen compounds (* exceeding the limit value)													
NO_2^-	mg/l	0.00	0.00	0.00	0.00	0.06	0.08	0.00	0.00	0.00	0.00	0.5	3
NH_4^+	mg/l	0.00	0.00	0.00	0.00	0.23	0.00	0.17	0.16	0.00	0.00	0.5	
NO_3^-	mg/l	2.48	7.34	13.44	3.93	64.09*	26.76	7.42	43.32	62.01*	9.83	50	50
Trace elements (* exceeding the limit value)													
Al	µg/l	438*	97	65	53	50	< 1	< 1	< 1	< 1	8		200
As	µg/l	1.9	5	2.8	2.8	8.1	8.3	3.9	4.1	6.3	15.8*	10	10
B	µg/l	10	17	13	15	66	66	8	19	19	229	1000	2400
Ba	µg/l	53.83	6.8	20.64	6.22	131.32	124.98	19.98	54.09	183.94	38.21	700	
Br	µg/l	14	12	18	15	61	59	21	88	104	75		
Cd	µg/l	0.06	< 0.05	< 0.05	< 0.05	< 0.05	< 0.05	< 0.05	< 0.05	< 0.05	< 0.05	5	3
Cr	µg/l	< 0.5	1.7	1.6	1.9	2.4	0.7	< 0.5	< 0.5	< 0.5	1.1	50	50
Cu	µg/l	3	0.6	1.4	0.4	0.5	0.8	0.6	0.7	0.6	1.5	2000	2000
Fe	µg/l	39	151	62	24	< 10	< 10	< 10	< 10	< 10	< 10	200	

Table 1 (continued)

Hg	µg/l	< 0.1	< 0.1	< 0.1	< 0.1	< 0.1	< 0.1	< 0.1	< 0.1	< 0.1	< 0.1		6
Mn	µg/l	128.51	17.22	3.28	1.2	0.48	0.17	0.32	0.14	0.16	1.64	50	400
Ni	µg/l	9.9	0.5	0.3	< 0.2	< 0.2	< 0.2	< 0.2	< 0.2	< 0.2	< 0.2	20	70
Pb	µg/l	< 0.2	< 0.2	74.9	< 0.2	0.6	< 0.2	< 0.2	< 0.2	< 0.2	< 0.2	25	10
U	µg/l	0.02	0.17	0.08	0.55	7.84	2.08	0.21	1.01	1.03	3.66		30
Sb	µg/l	< 0.5	< 0.05	0.11	0.08	0.05	< 0.05	< 0.05	< 0.05	0.05	0.22	5	20
Se	µg/l	< 0.5	< 0.5	< 0.5	< 0.5	0.6	< 0.5	< 0.5	0.6	0.6	0.9	10	40
Zn	µg/l	37.8	2	5.4	4.8	1.6	1.6	2.8	6.1	3.9	5.6		
Isotopic characteristics													
Oxygen-18 (δ ^{18}O)	‰ SMOW	− 11.08	− 11.28	− 11.26	− 11.24	− 8.91	− 10.32	− 11.56	− 10.72	− 9.72	− 10.55		
Deuterium (δ ^{2}H)	‰ SMOW	− 73.83	− 73.49	− 72.86	− 73.9	− 68.75	− 72.38	− 77.2	− 74.32	− 65.96	− 71.64		
Tritium (^{3}H)	TU	1.85	3.01	4.87	4.88	3.94	2.30	4.35	5.04	4.80	0.96	11.83	
^{3}H error		± 0.82	± 0.84	± 0.90	± 0.86	± 0.88	± 0.82	± 0.84	± 0.88	± 0.90	± 0.78		
d-Excess = δ^{2}H − 8δ^{18}O	‰	14.81	16.75	17.22	16.02	2.53	10.18	15.28	11.44	11.8	12.76		

Fluoride-rich minerals are most abundant in almost all rocks (Saxena and Ahmed 2001). The geological formation of this region (Davulga village) is mainly conglomerate, sandstone, marl, and limestone, followed by tuff-tuffite–marl, and covered clayey limestone.

Hydrochemical facies evaluations define the complex hydrochemical processes in the subsurface (Kumar 2013). Hydrogeochemical facies evaluates geochemical classification of waters and interpretation of chemical data. To determine hydrogeochemical facies, Piper (1944) trilinear and semilogarithmic Schoeller (1962) diagrams were used, and Gibbs (1970) plots were also evaluated for understanding the dominant factors in the spring waters. According to the Piper diagram, the springs are generally "$CaMgHCO_3$"-type waters, but the Emirdağ spring water is of the "$CaMgSO_4$" type (Fig. 2). The semilogarithmic Schoeller (1962) diagram indicated that spring waters except for the Emirdağ spring have similar lithologic origin and the same recharge area (Fig. 3). According to the diagram, the spring waters are generally Ca^{2+} and HCO_3^- ion-rich waters.

Gibbs plot (Fig. 4) is used to know the association of groundwater composition with the aquifer lithology and represent the source of chemical constituents in groundwater such as precipitation, rock, and evaporation dominance (Gibbs 1970). The ratios for cations and anions, i.e., Na/(Na + Ca) and Cl/(Cl + HCO_3), and of the groundwater samples when plotted against relative values of TDS showed the "water–rock interaction zone" dominance process in the spring samples. The geological formations, water–rock interaction, and relative mobility of ions influenced the geochemistry of groundwater (Yousef et al. 2009). The hydrochemical facies of the spring waters in the investigation area is controlled by rock–water interaction.

Hydrogeochemical process

The hydrochemical processes can be explained with ion exchange, mineralization, weathering, and dissolution. Results from the chemical analyses were used to identify the hydrogeochemical processes. The chemical composition of water, ion exchange, mineralization, weathering, and dissolution can be explained by the hydrochemical processes. Also, the plotted *X*–*Y* coordinate defines the geochemical variations of groundwater (Güler et al. 2002). Results of the chemical analyses in water were used to identify hydrogeochemical processes.

Ion exchange

The ion exchange can be determined with chloroalkaline indices to groundwaters. Chloroalkaline indices I and II (CAI-I and CAI-II) are calculated from the following Eqs. (1) and (2):

Fig. 2 Piper diagram

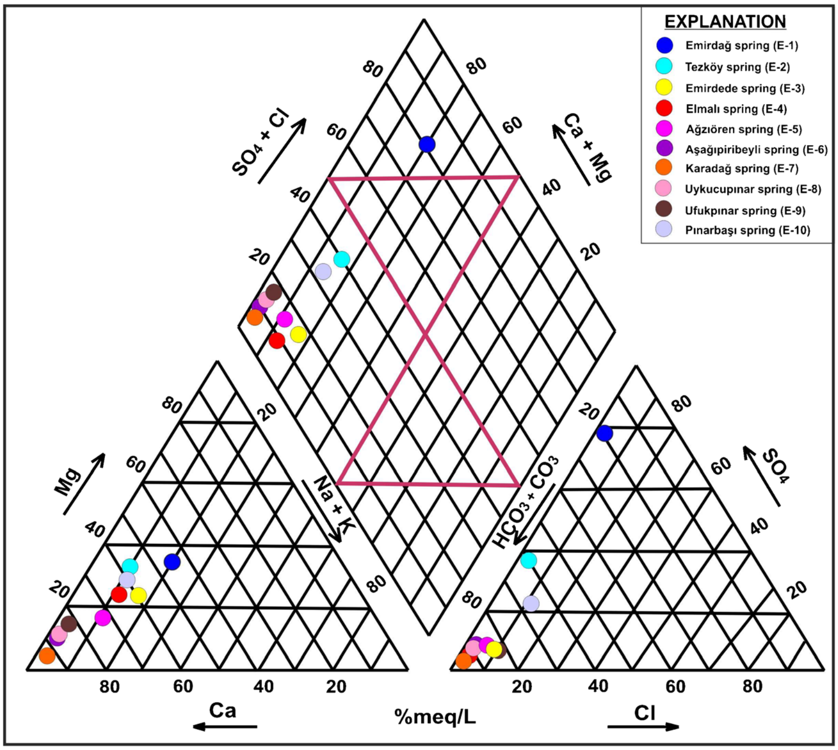

$$\mathrm{CAI{-}I} = [\mathrm{Cl}^{-}(\mathrm{Na}+\mathrm{K})]/\mathrm{Cl} \quad (1)$$

$$\mathrm{CAI{-}II} = [\mathrm{Cl}^{-}(\mathrm{Na}+\mathrm{K})]/(\mathrm{SO}_4+\mathrm{HCO}_3+\mathrm{CO}_3+\mathrm{NO}_3) \quad (2)$$

(All values are expressed in meq/l).

When there is an exchange between Na^+ or K^+ with Mg^{2+} or Ca^{2+} in the groundwater, both the above indices will be positive, and if there is a reverse ion exchange prevalent, then both these indices will be negative (Schoeller 1965). In spring waters, CAI-I values range from − 10.69 to − 0.53, while CAI-II values range from − 0.22 to 0.02 (Table 1, Fig. 5a). All the computed values of CAI were negative and there is a reverse ion exchange, thus indicating exchange of Mg^{2+} and Ca^{2+} of the water with Na^+ and K^+ of the rocks.

Carbonate weathering

The concentrations of Ca^{2+} and Mg^{2+} ions range from 11.43 to 148.32 mg/l and from 2.80 to 41.78 mg/l, respectively. The concentrations of SO_4^{2-} and HCO_3^- range from 2.89 to 152.23 mg/l and from 18.30 to 488.00 mg/l, respectively. Mg^{2+} and Ca^{2+} were the dominant cations present in the spring waters in the investigation area. Similarly, HCO_3^- was also present in significant amounts. This situation is mostly due to weathering of calcium and bicarbonate minerals and leaching of limestones.

Figure 5 shows the scatter plots of (Ca^{2+} + Mg^{2+}) versus (HCO_3^- + SO_4^{2-}) indicating that 60% of the samples lie above the equiline of 1:1 and that there is a very strong correlation R^2 = 0.98 ($Ca^{2+} + Mg^{2+} = 1.0069 \times SO_4^{2-} + HCO_3^- + 0.1795$), thus indicating carbonate weathering except for the E-1, E-2, E-4, and E-10 samples (Fig. 5b). In the scatter plots, the ionic concentrations falling above the equiline result from carbonate

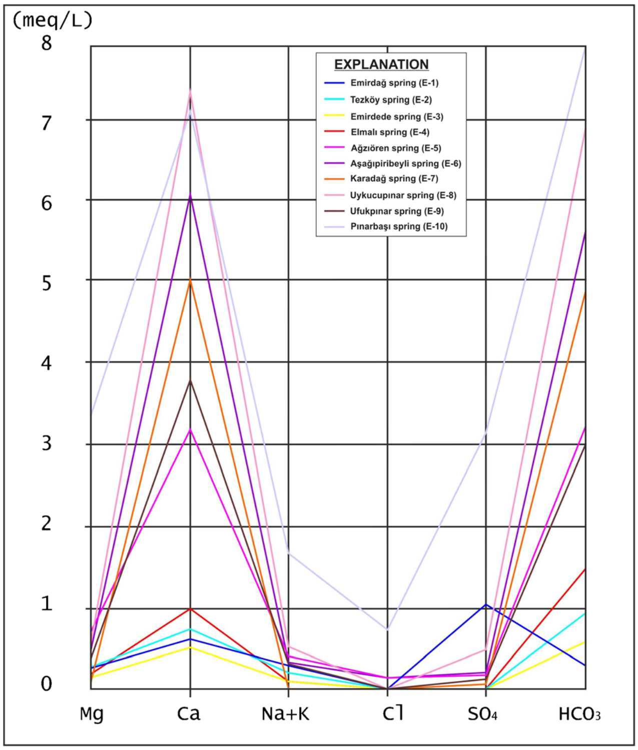

Fig. 3 Semilogarithmic Schoeller diagram

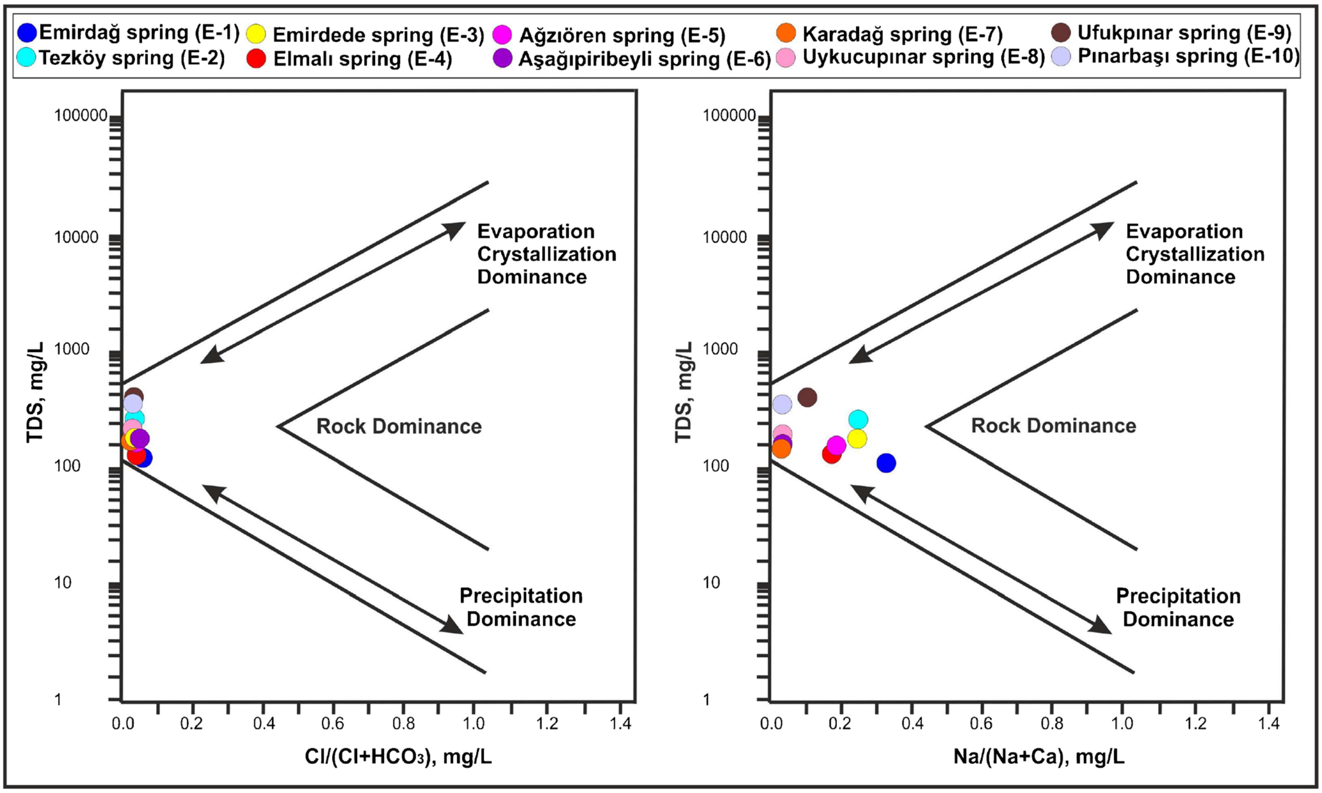

Fig. 4 Gibbs diagram

weathering (Dehnavi et al. 2011). Carbonate weathering results from the action of rainwater impregnated with CO_2 and becomes rich in carbonic acid (Nayak and Sahood 2011). Carbonic acid influences the dissolution of carbonate minerals (calcite and dolomite) in the aquifer system (Nur et al. 2012). The Midos, Loras, and Piribeyli formations are the major sources of carbonate in the investigation area. Carbonate minerals are dissolved when the waters contact with calcium and carbonate-rich minerals in karstic units of the investigation area.

The chemical data of the groundwater samples is plotted for the $Ca^{2+} + Mg^{2+}$ versus $HCO_3^- + CO_2^{3-}$ diagram (Fig. 5c). The data fall below the equiline 1:1, which suggests that an excess of alkalinity in the water has been balanced by alkalis ($Na^+ + K^+$).

The dissolution of calcite and dolomite in the aquifer was shown with the plot of Ca/Mg ratio of groundwater. That is, if the ratio Ca/Mg = 1, dissolution of dolomite should occur, whereas a higher ratio is indicative of greater calcite contribution (Maya and Loucks 1995). Higher Ca/Mg ratio > 2 indicates the dissolution of silicate minerals, which contribute calcium and magnesium to groundwater. It can be seen from Fig. 5 d that the spring water samples in the investigation area were found to have values greater than 2 (Table 1), indicating the effect of silicate minerals.

Silicate weathering

Silicate weathering can be estimated according to the ratio between ($Na^+ + K^+$) and total cations (TC^+). The relationship in the investigation area indicates that all of the samples are plotted above the $Na^+ + K^+ = 0.5\ TC^+$ line (Fig. 5e), which reflects the involvement of silicate weathering in the geochemical processes, contributing mainly sodium and potassium ions to groundwater (Stallard and Edmond 1983).

A further plot of $Ca^{2+} + Mg^{2+}$ versus total cations (TC^+) in spring water samples is shown in Fig. 5 f which resulted in a linear spread between $Ca^{2+} + Mg^{2+} = 0.5\ TC^+$ line and $Ca^{2+} + Mg^{2+} = TC^+$, indicating that the increase in $Ca^{2+} + Mg^{2+}$ ions results from the weathering of silicate minerals. The dominant hydrochemical facies of springs was $CaMgHCO_3$, reflecting the influence of silicate weathering. The increased contribution of alkalis to the major ions is caused by silicate weathering (Rao 2008).

Correlation analysis

Correlation matrix has been effectively and extensively employed in understanding relationships among constituent parameters in groundwater (Omonona et al. 2013; Onwuka and Omonona 2017; Tiwari et al. 2017; Amano et al. 2018).

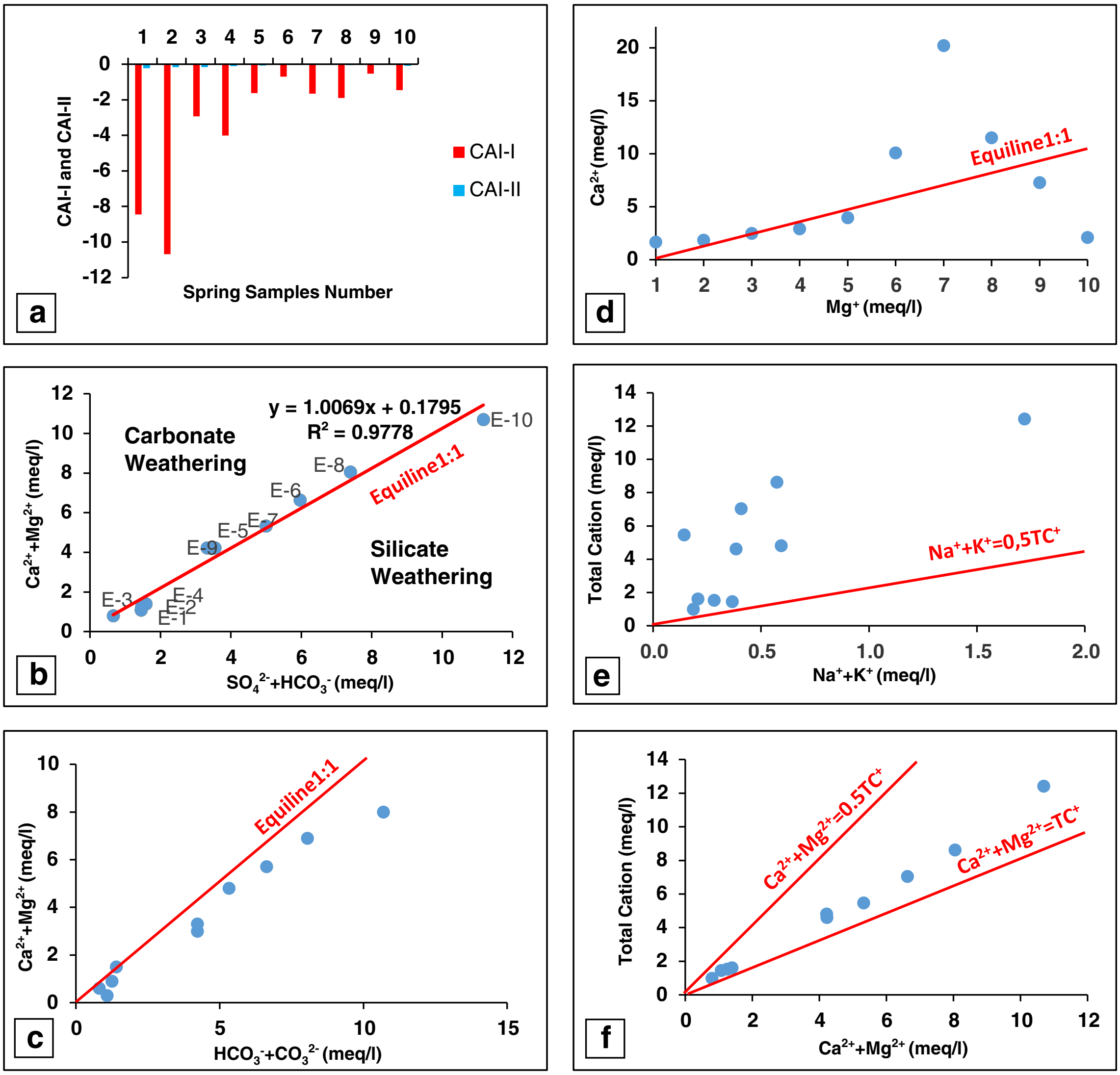

Fig. 5 Scatter diagram of relation parameters of spring waters. **a** Bar diagram of chloroalkaline indices (CAI-I and CAI-II). **b** Relation between Ca^{2+} + Mg^{2+}–SO_4^{2-} + HCO_3^-. **c** Relation between Ca^{2+} + Mg^{2+}–HCO_3^- + CO_2^{3-}. **d** Relation between Ca^{2+}–Mg^{2+}. **e** Relation between TC^+–Na^+ + K^+. **f** Relation between TC^+–Ca^{2+} + Mg^{2+}

Various methods in correlation analysis are used to identify the relation between hydrochemical variables. Correlation coefficient $p < 0.05$ of variables is a significant level. A good relationship between two variables has high correlation coefficient (near 1 or 1); if there is no relationship, the value is 0. The relationships between various elements were carried out using Spearman's correlation analysis (Table 2). A strong positive and significant Spearman's correlation coefficient ($p < 0.01$) was found between most physical parameters and major elements.

Various indices were calculated for determining the irrigation water quality for parameters such as EC, TDS, total hardness (TH), Na%, SAR, SH, RSC, RSBC, PI, potential salinity (PS), SSP, MR, KR, synthetic harmful coefficient (K), and Ka. The springs are classified according to the irrigation water criteria. Also, chloroalkaline indices (CAI-I and CAI-II) were calculated.

EC was related to K^+ and HCO_3^- ions with correlation coefficients of 0.588 and 0.515, respectively. The moderate correlations reflected significant contributions of these ions to groundwater mineralization. There was relation between temperature and K^+ ($r = 0.511$). There was a strong correlation between pH and SO_4^{2-} ($r = 0.927$) and pH and HCO_3^- ($r = 0.709$). TDS was related to chloride and arsenic with correlation coefficients of 0.539 and 0.644, respectively, and this significant correlation depends on anthropogenic pollution sources. The results are shown in Table 2. There is a strong positive correlation with cations (Na^+, Ca^{2+}, Mg^{2+}, K^+) and anions (Cl^-, SO_4^{2-}, HCO_3^-), which indicates that they may be derived from rock–water interaction processes and ionic

Table 2 Spearman correlation coefficients of variables taken for spring waters

	T	EC	pH	TDS	Na^+	K^+	Mg^{2+}	Ca^{2+}	Cl^-	SO_4^{2-}	HCO_3^-	NO_3^-	Al	As
T	1.000													
EC	0.249	1.000												
pH	− 0.553	− 0.442	1.000											
TDS	− 0.176	0.455	− 0.018	1.000										
Na^+	0.316	0.224	− 0.455	0.406	1.000									
K^+	0.480	0.588*	− 0.927*	0.285	0.661*	1.000								
Mg^{2+}	0.377	0.370	− 0.418	0.430	0.964*	0.648*	1.000							
Ca^{2+}	0.182	0.406	− 0.103	0.467	0.552*	0.297	0.661*	1.000						
Cl^-	− 0.024	0.115	0.030	0.539*	0.673*	0.139	0.661*	0.709*	1.000					
SO_4^{2-}	0.511*	0.333	− 0.709*	0.394	0.600*	0.818*	0.600*	0.309	0.152	1.000				
HCO_3^-	0.195	0.515*	− 0.079	0.455	0.564*	0.285	0.685*	0.964*	0.758*	0.224	1.000			
NO_3^-	− 0.517	0.006	0.224	0.430	0.552*	− 0.006	0.527	0.430	0.697*	− 0.152	0.467	1.000		
Al	0.260	− 0.075	− 0.331	− 0.450	− 0.256	0.175	− 0.338	− 0.838	− 0.732	0.100	− 0.788	− 0.607	1.000	
As	0.171	0.462	− 0.079	0.644*	0.705*	0.322	0.809*	0.632*	0.778*	0.340	0.723*	0.590*	− 0.508	1.000

*Correlation is significant at the $p < 0.01$ level

exchange. Na^+ exhibited a strong correlation with K^+ (r = 0.661), Mg^{2+} (r = 0.964), Cl^- (r = 0.673), and SO_4^{2-} (r = 0.600) and a moderate correlation with Ca^{2+} (r = 0.552), HCO_3^- (r = 0.564), and NO_3^- (r = 0.552). Groundwater from basalt aquifers displays positive correlations between major cations (Na^+, Ca^{2+}, and Mg^{2+}) and alkalinity (HCO_3^-) (Kortatsi 2006). The basaltic volcanic rocks in the springs and in the vicinity of the investigation area are very widespread. K^+ was strongly correlated with Mg^{2+} and SO_4^{2-} with correlation coefficients of 0.648 and 0.818. Mg^{2+} was related to the ions (Ca^{2+}, Cl^-, SO_4^{2-}, and HCO_3,) and As with strong correlation coefficients of 0.661, 0.661, 0.600, 0.685, and 0.809, respectively. There was a strong correlation between Ca^{2+} and anions (Cl^-, HCO_3^-) (r = 0.709, r = 0.964). Cl^- and HCO_3^- have a strong correlation (r = 0.758). There was a positive and significant correlation between NO_3^-, As, Na^+, and Cl^-. Nitrate was related to arsenic with correlation coefficients of r = 0.590, and the significant correlation originates from the water–rock interaction and anthropogenic pollution. NO_3^-–Na^+ ratio ≥ 0.5 was observed to have a positive correlation (r = 0.552) and NO_3^-–Cl^- was observed to have a very strong correlation (r = 0.697) in samples with NO_3^- levels above 50 mg/l, indicating likely from on-site and agricultural sources. Nitrate concentrations of the Ağzıören (64.09 mg/l) and Ufukpınar (62.01 mg/l) springs were determined to be above the drinking limit value due to agricultural sources. The high correlation between As–TDS (r = 0.644), As–Na^+ (r = 0.705), As–Mg^{2+} (r = 0.809), As–Ca^{2+} (r = 0.632), As–Cl^- (r = 0.778), As–HCO_3^- (r = 0.723), and As–NO_3^- (r = 0.590) are attributed to rock–water interaction processes. Pınarbaşı spring arsenic concentration (15.8 mg/l) may exceed the drinking water limit value from rock–water interaction.

Drinkability of the springs

The major cation–anion concentrations (Ca^+, Mg^+, Na^+, K^+) in the spring waters are below the WHO (2011) standards. The Schoeller diagram was used to determine the drinkability of the spring waters in the investigation area. According to the diagram, Tezköy, Aşağıpiribeyli, Uykucupınar, and Pınarbaşı spring waters are in the class of "good quality" and the other spring waters have "very good quality waters" (Fig. 6). In addition, the physical properties and major ions of all samples were within the WHO (2011) and TS-266 (2005) permissible limits for drinking water.

Irrigation usability of springs

To know the suitability of groundwater quality for irrigation is very essential and useful for Emirdağ region because the people in the region are provided livelihood through agricultural activities. The springs in the region have been evaluated in detail in terms of irrigation water quality. Especially, the US Salinity Laboratory (USSL) and Wilcox diagrams were implemented, and these methods were used to determine EC, TDS, TH, Na%, SAR, salinity hazard (SH), RSC, RSBC, PI, PS, SSP, MR, KR, K, and Ka. The data obtained was evaluated according to the irrigation classifications in Table 3, and spring waters are suitable for irrigation in the Emirdağ region.

The US Salinity Laboratory (Richards 1969) and Wilcox (1955) diagrams were used to determine the availability of spring waters for irrigation purposes in agricultural areas. According to the US Salinity Laboratory diagram, generally, spring waters are in the class of "C_2S_1," i.e., medium salinity

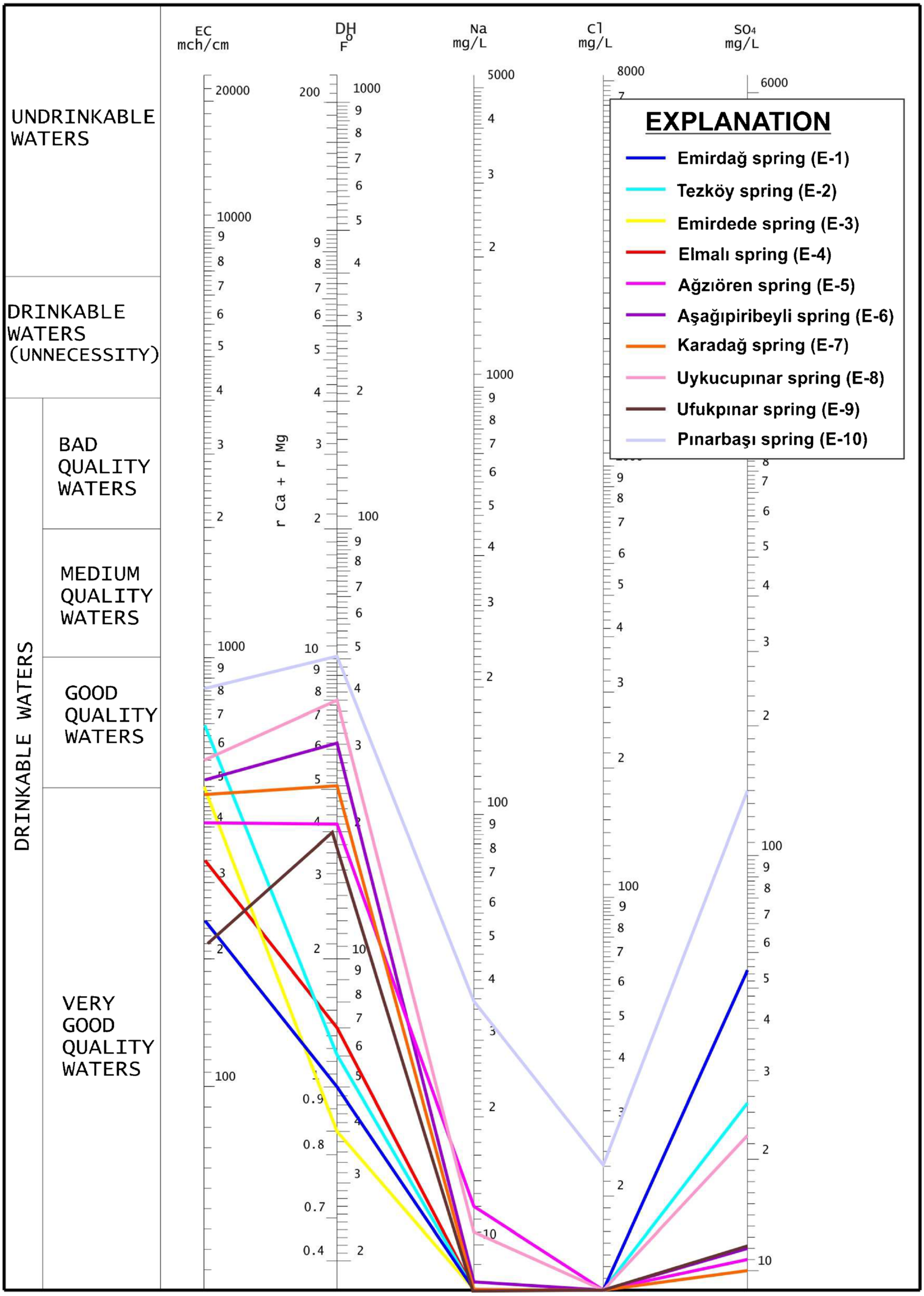

Fig. 6 Schoeller diagram

waters with low sodium. But, Emirdağ spring water has low salinity with water having low sodium “C_1S_1” and Pınarbaşı spring water is “C_3S_1,” i.e., high salinity with low sodium water, and occasional soil washing measures should be taken to prevent salting and salt-sensitive plants should not be grown (Fig. 7). In the Wilcox diagram, all spring waters are “very well-usable” in the investigation area (Fig. 8).

The EC values of springs range from 240 to 790 μS/cm (Table 1). Also, according to EC, 90% of the spring samples are suitable for irrigation. Springs are “good and excellent” based on electrical conductivity classification by Richard (1984) and Raghunath (1987) except one sample (Table 3). Pınarbaşı spring is “doubtful” due to its EC value of 790 μS/cm (EC > 750 μS/cm). The TDS values in the study area vary from 90 to 132 mg/l (Table 1). Also, according to TDS classification, 100% of the springs are suitable for irrigation. Spring water samples falls under “freshwater” (TDS < 1.000 mg/l) types of water (Catroll 1962; Freeze and Cherry 1979; Table 3). The average total hardness (as $CaCO_3$) of the springs in the study area ranges from 40.02 to 534.68 mg/l (Table 1). Emirdağ, Tezköy, Elmalı, and Dedeköy spring samples were “soft” and suitable for irrigation. Ağzıören, Karadağ, and Ufukpınar spring samples were “hard,” and Aşağıpiribeyli, Uykucupınar, and Pınarbaşı spring samples were determined to be “very hard” according to Sawyer and McMcartly (1967). The springs exceeding the limit of 300 mg/l were unsuitable for irrigation. The Na% values range from 2.63 to 25.43% (Table 1). According to Na% classification, springs are “good and excellent” (Table 3). Also, according to the related percentage sodium and total concentration (Wilcox 1955), the

Fig. 7 US Salinity Laboratoy diagram

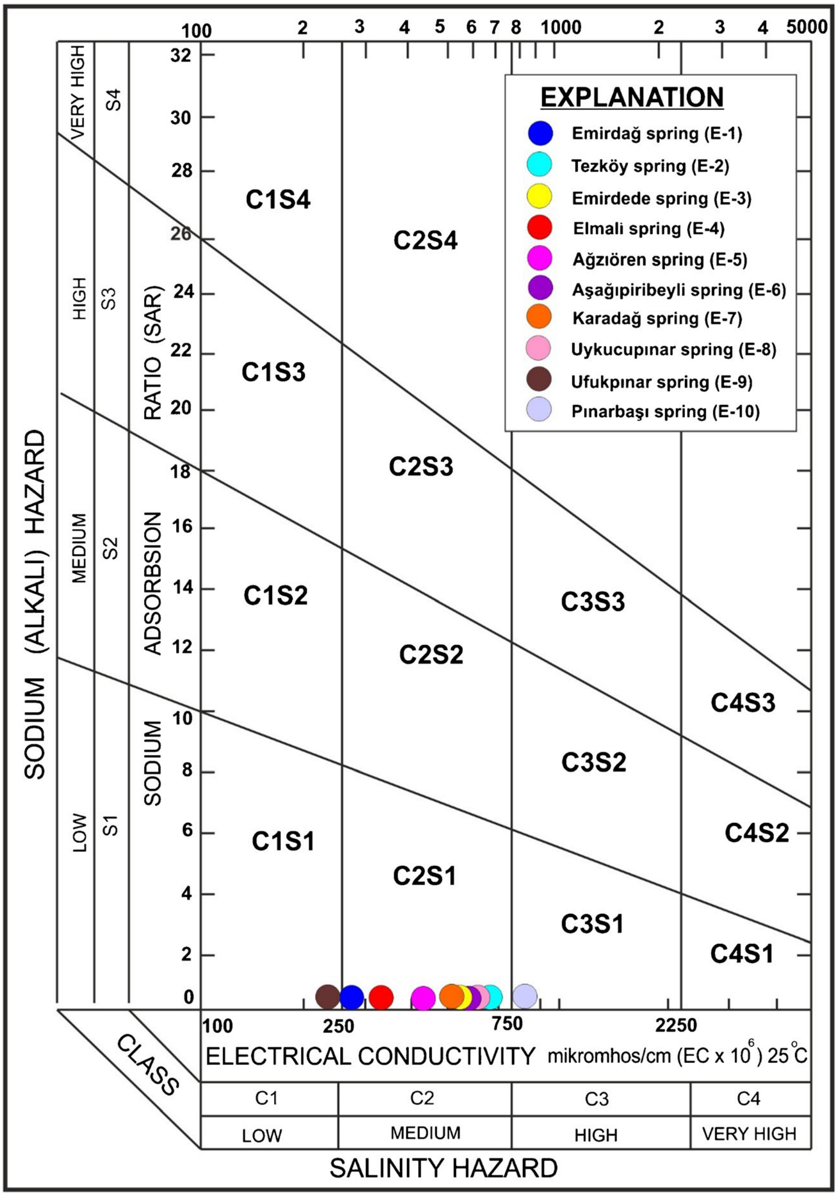

Fig. 8 Wilcox diagram

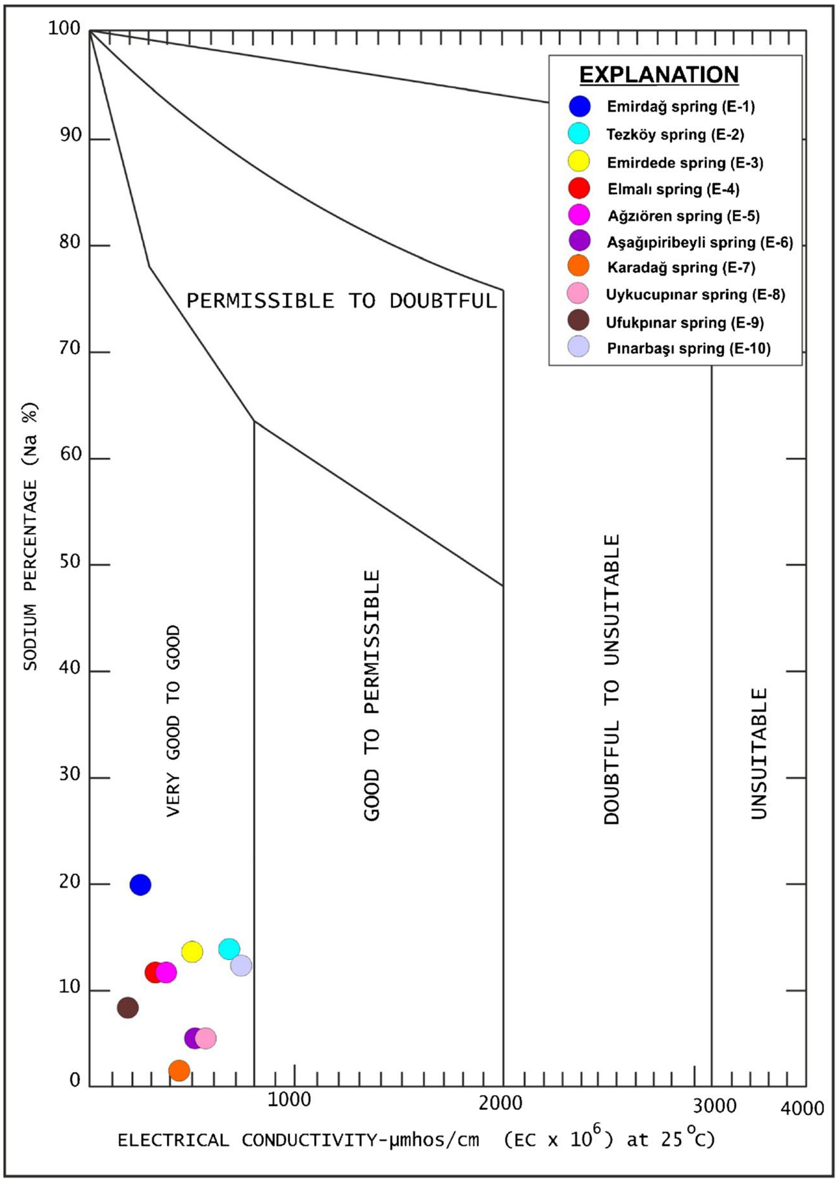

spring samples are "very well-usable" and the springs are suitable for irrigation. The SAR values range from 0.05 to 0.55 meq/l in the spring samples (Table 1). According to the SAR classification (Richards 1954; Todd 1980; Karanth 1987; Saleh et al. 1999), spring waters in the study area were determined "excellent" because its SAR values are < 10 meq/l. Also, according to the salinity hazard classification (Richard 1954), spring waters are "good and excellent" except Pınarbaşı spring quality due to electrical conductivity value of 790 μS/cm (Table 3). The RSC values are from − 2.69 to 0.10 (Table 1). Spring samples are "good" (Eaton 1950; Richards 1954; Raghunath 1987; Table 3). The RSBC values of the spring samples from the study area vary from − 0.71 to 0.74 meq/l (Table 1). As per the classification of Gupta (1983) and Gupta and Gupta (1987), all spring samples are "satisfactory" (< 5 meq/L) for irrigation (Table 3). The PI values range between 36.12 and 97.29 meq/l (Table 1). The resulting spring samples are class I and class II according to Doneen (1964) and samples can be categorized as "good and excellent" (Doneen 1964; Domenico and Schwartz 1990, Table 3). The PS of the water samples varied from − 0.88 to 0.11 meq/l (Table 1). As per Doneen (1962), the classification of all spring samples is "excellent to good" (< 5 meq/l) for irrigation (Table 3). The SSP values range from 2.57 to 25.99 meq/l (Table 1) and spring samples are "excellent to good" for irrigation water (Table 3). The MR was found in the range from 4.71 to 37.40 meq/l (Table 1) in the spring samples, and these spring waters are "suitable" due to MR < 50 meq/l for irrigation in the study area (Table 3). The KR was found in the range from 0.03 to 0.28 meq/l in spring samples (Table 1). All spring waters are "suitable" for KR < 1 meq/l for irrigation in the investigation area (Table 3). Synthetic harmful coefficient

Table 3 Irrigation water classifications of the springs

PARAMETER	SYMBOL	UNIT	REFERENCES	FORMULA	RANGES	WATER CLASS		SAMPLE NO
Electrical Conductivity	EC	µS/cm	Richard 1954 Raghunath 1987		<250	Excellent		9
					250-750	Good		1,2,3,4,5,6,7,8
					750-2000	Permissible		10
					2000-3000	Doubtful		
					>3000	Unsuitable		
Total Dissolved Solids	TDS	mg/L	Catroll 1962 Freeze and Cherry 1979	$TDS=0.64xEC$	<1.000	Fresh water		1,2,3,4,5,6,7,8,9,10
					1.000-10.000	Brackish water		
					10.000-100.000	Saline water		
					>100.000	Brine water		
Total Hardness	TH	mg/L $CaCO_3$	Sawyer and McMcartly1967	$TH=(Ca^{2+}+Mg^{2+})meq/Lx50$	<75	Soft		1,2,3,4
					75-150	Moderately hard		
					150-300	Hard		5,7,9
					>300	Very hard		6,8,10
Percentage Sodium	Na%	meq/L	Wilcox 1955	$Na\%=\{(Na^{+}+K^{+})x100\}/(Ca^{2+}+Mg^{2+}+Na^{+}+K^{+})$	0-20	Excellent		1
					20-40	Good		2,3,4,5,6,7,8,9,10
					40-60	Permissible		
					60-80	Doubtful		
					>80	Unsuitable		
Sodium Adsorption Ratio	SAR	meq/L	Todd 1980 Richards 1954 Saleh et al. 1999	$SAR=Na^{+}/\{(Ca^{2+}+Mg^{2+})/2\}$	<10	Excellent	S1	1,2,3,4,5,6,7,8,9,10
					10-18	Good	S2	
					19-26	Doubtful	S3	
					>26	Unsuitable	S4-S5	
Salinity Hazard	SH		Richards 1954		100-250 (EC)	Excellent	C1	1
					250-750	Good	C2	2,3,4,5,6,7,8,9
					750-2250	Doubtful	C3	10
					>2250	Unsuitable	C4-C5	
Residual Sodium Carbonate	RSC	meq/L	Eaton 1950 Richards 1954 Raghunath 1987	$RSC=(HCO_3^{-}+CO_3^{2-})-(Ca^{2+}+Mg^{2+})$	<1.25	Good		1,2,3,4,5,6,7,8,9,10
					1.25-2.5	Doubtful		
					>2.5	Unsuitable		
Residual Sodium Bicarbonate	RSBC	meq/L	Gupta 1983	$RSBC=(HCO_3^{-}-Ca^{2+})$	<5	Satisfactory		1,2,3,4,5,6,7,8,9,10
					5-10	Marginal		
					>10	Unsatisfactory		
Permeability Index	PI	meq/L	Raghunath 1987	$PI=\{(Na^{+}+\sqrt{HCO_3^{-}})x100\}/(Na^{+}+Ca^{2+}+Mg^{2+})$	>75%	Excellent	Class I	2,3,4
					75% - 25%	Good	Class II	1,5,6,7,8,9,10
					<25%	Unsuitable	Class III	
Potential Salinity	PS	meq/L	Doneen 1962	$PS=(Cl^{-})-(½SO_4^{2-})$	<5	Excellent to good		1,2,3,4,5,6,7,8,9,10
					5-10	Good to injurious		
					>10	Injurious to satisfactory		
Soluble Sodium Percentage	SSP	meq/L	Todd 1960	$SSP=\{(Na^{+})/(Ca^{2+}+Mg^{2+}+K^{+})\}x100$	0-20	Excellent		2,3,4,5,6,7,8,9,10
					20-40	Good		1
					40-60	Permissible		
					60-80	Doubtful		
					80-100	Unsuitable		
Magnesium Ratio	MR	meq/L	Raghunath 1987	$MR=(Mg^{2+}x100)/(Ca^{2+}+Mg^{2+})$	<50	Suitable		1,2,3,4,5,6,7,8,9,10
					>50	Unsuitable		
Kelly's Ratio	KR	meq/L	Kelly 1963	$KR=\{(Na^{+})/(Ca^{2+}+Mg^{2+})\}$	<1	Suitable		1,2,3,4,5,6,7,8,9,10
					1-2	Marginal suitable		

Table 3 (continued)

PARAMETER	SYMBOL	UNIT	REFERENCES	FORMULA	RANGES	WATER CLASS	SAMPLE NO
					>2	Unsuitable	
Synthetic harmful coefficient	K	meq/L	Xu et al. 2019	K=12.4M+SAR M=where M represents the total dissolved solids (in g/L)	K<25	Excellent	1,2,3,4,5,6,7,8,9,10
					25<K<36	Good	
					36<K<44	Injurious	
					K>44	Unsuitable	
Irrigation coefficient	Ka	meq/L	Xu et al. 2019	$Ka=288/(5Cl^-)$ if $Na^+<Cl^-$ $288/(Na^++4Cl^-)$ if $Cl^-<Na^+<Cl^-+2SO_4^{2-}$ $288/(10Na^+-5Cl^--9SO_4^{2-})$ if $Na^+>Cl^-+2SO_4^{2-}$	>18	Excellent	1,2,3,4,5,6,7,8,9,10
					6-18	Good	
					1.2-6	Doubtful	
					>1.2	Unsuitable	

(K) can comprehensively reflect the salt and alkali hazards. K values of the spring samples ranged from 1.64 to 6.08 meq/l (Table 1). The samples were classified as "excellent" (Xu et al. 2019) and the waters are suitable for irrigation (Table 3). Irrigation coefficient (Ka) can be determined depending on the Na^+, Cl^-, and SO_4^{2-} ions in the water. Ka values ranged from 65.17 to 895.55 meq/l, and according to the Ka classification (Xu et al. 2019), the average level was "excellent" for the spring samples (Table 1 and Table 3). All methods and formulas required for irrigation classification are presented in detail in Table 3.

Water pollution in the springs

The livelihood of the people in the investigation area is agriculture. The analysis results of nitrogen compounds (NO_3^-, NO_2^-, and NH_4^+) were evaluated in order to determine their effect on spring waters of substances like pesticides, fertilizers, etc. used in agriculture. In addition, analyses of trace elements (Al, As, B, Ba, Br, Cd, Cr, Cu, Fe, Hg, Li, Mn, Ni, Pb, U, Sb, Se, and Zn) were also evaluated (Table 1).

Nitrogen compounds The nitrate, nitrite, and ammonium concentration changes in the investigation area are 2.74–10.76, 0–0, and 0.03–0.47 mg/l, respectively (Table 1). Nitrite and ammonium concentrations of waters were within the recommended values for drinking water (WHO 2011). However, the concentration of nitrate in the Ağzıören (64.09 mg/l) and Ufukpınar (62.01 mg/l) springs exceeds the drinking water standard limit (50 mg/l). Nitrate originates from both natural and anthropogenic sources. Nitrogen comprises 78% of the earth's atmosphere, and the cycling of nitrogen in the ecosystem is affected by both biotic and abiotic processes (Bouchard et al. 1992). The nitrates are mainly attributed from domestic waste, animal wastages, nitrogen-rich fertilizers, etc. (Wagh et al. 2019a, b). Especially, high levels of nitrate in groundwater are usually the result of improper disposal of human wastes, especially by septic tanks, industrial and food processing operations, and silvicultural or agricultural activities.

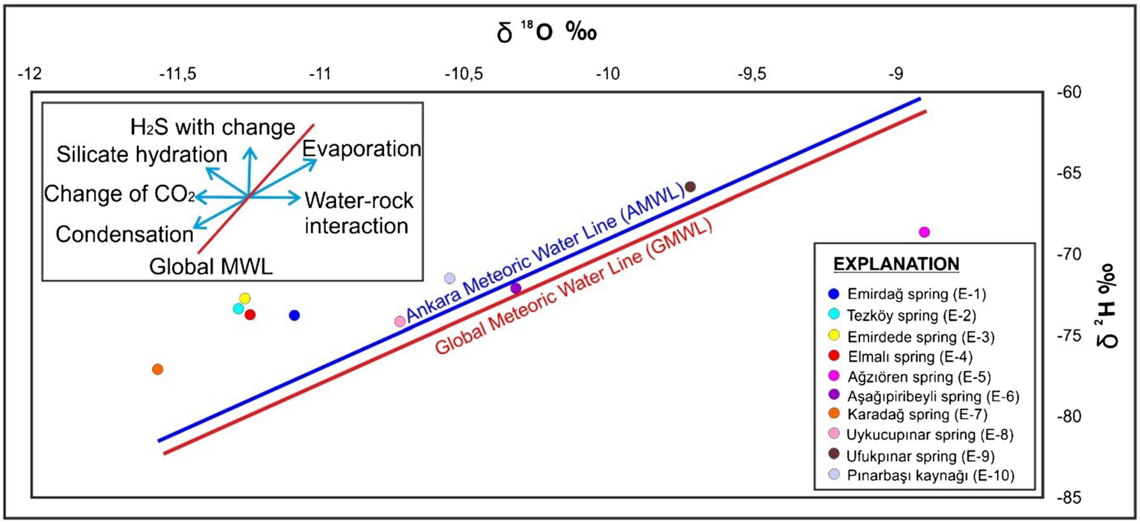

Fig. 9 Plot of δ^2H and $\delta^{18}O$ for spring waters

Fig. 10 Tritium versus oxygen-18 isotope values of spring waters

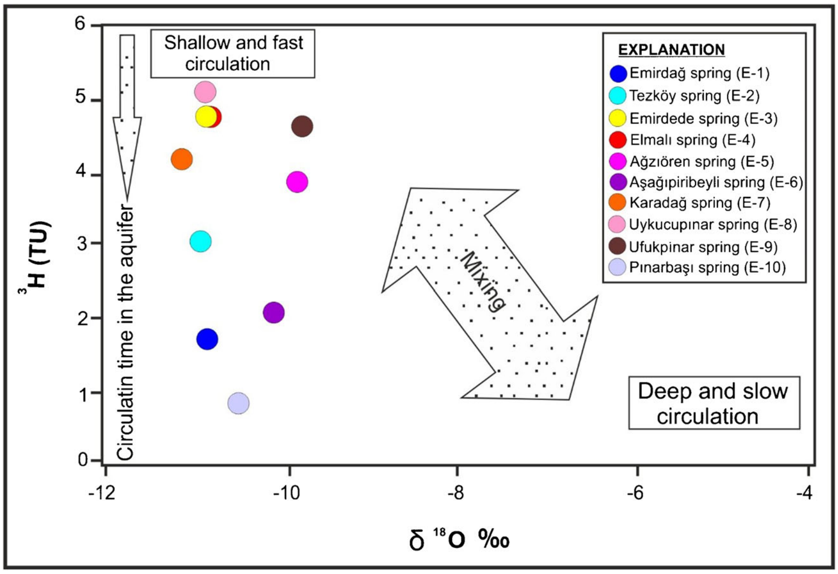

Nitrate also occurs naturally in geological deposits of nitrate salts as sodium nitrate; some of these deposits were an important source of fertilizer prior to the emergence of synthetic nitrogen fertilizer (Barbieri et al. 2019). Also, nitrate is a source for plants and is commonly used as a fertilizer (Fedkiw 1991). Ağzıören (64.09 mg/l) and Ufukpınar (62.01 mg/l) spring samples were collected in an area with agricultural activities, so the nitrate concentrations could be related to contamination by excessive use of fertilizers in the field, thereby causing health problems. Nitrate is one of the main groundwater pollutants; high nitrate concentrations in groundwater can cause public health risks and environmental pollution that

Fig. 11 d-Excess (‰) versus Cl$^-$ (mg/l), EC (μS/cm), and δ^{18}O in relation to spring waters

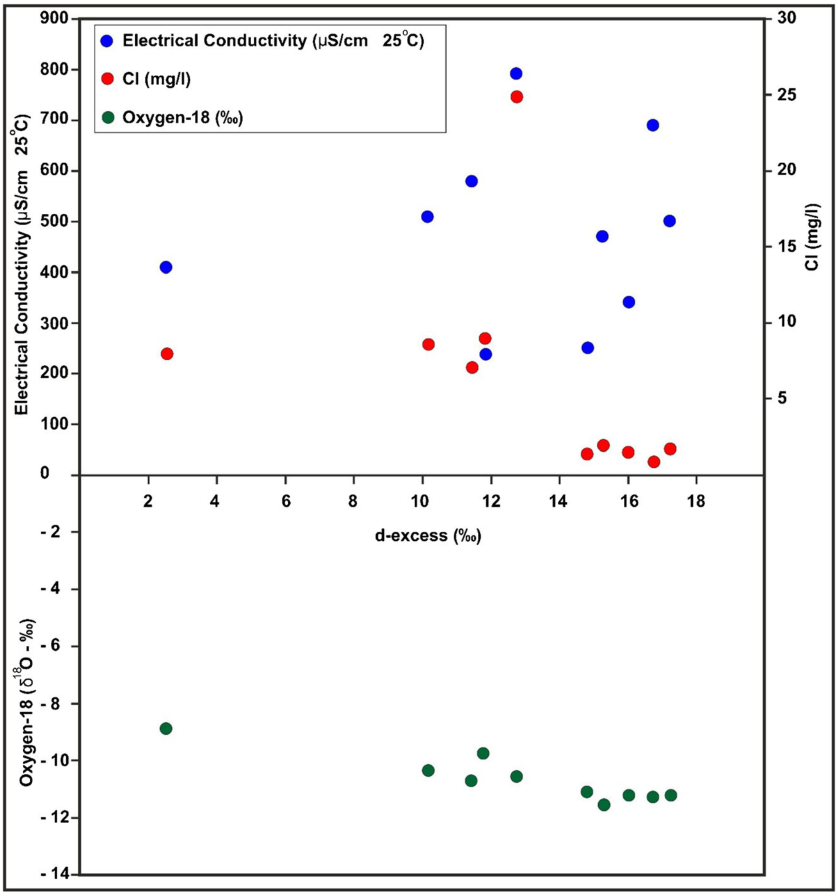

have already become a common problem in many parts of the world. The threat from nitrate depends on its scales, which can take on chronic or acute forms (Sousa et al. 2014). The consumption of nitrate-rich water leads to methemoglobinemia and affects oxygen circulation in the blood. Also, it causes the blue-baby syndrome in infants as well as hypertension and stomach cancer (Comly 1945).

Trace elements Generally, trace element concentration values except for aluminum and arsenic do not exceed these limit values of the drinking water standards of WHO (2011) and TS-266 (2005). According to TS-266 (2005) and U.S. EPA (2012) drinking water standards, the maximum allowable limits of aluminum is 200 μg/l. Al contents determined in the investigation area range from > 1 to 438 μg/l. The highest Al content was determined at Emirdağ spring (438 μg/l) discharged from volcanic rocks near Emirdağ district. Feldspar, kaolin, and mica minerals in volcanic units are caused by Al concentration increase of groundwater due to rock–water interaction (Erikson et al. 1981).

Arsenic concentrations measured in the study area range from 1.9 to 15.8 μg/l. The permissible limit from the TS-266 (2005) and WHO (2011) drinking water standards for maximum arsenic concentrations in groundwater is 10 μg/l. Arsenic concentration (15.8 μ/l) at the Pınarbaşı spring exceeds the drinking water standards limits of WHO (2011) and TS-266 (2005). Sediments derived from volcanic rocks generally have higher arsenic concentrations (Saldivar and Soto 2009). The dominant source of arsenic in the spring from the study area is related to the geological setting. Miocene aged Köroğlu volcanic rocks outcrop in a wide area of the region. The Pınarbaşı spring is discharged from the Köroğlu volcanic rocks. The arsenic concentration increase can be ascribed to the water–rock interaction with the volcanic rocks. The increase in arsenic concentration in drinking water is dangerous to human health. The water demand for drinking and agricultural purposes by the people living in the villages in the study area is not taken from the rocks.

Isotopic characteristics in the springs

The environmental isotopes of oxygen-18 ($\delta^{18}O$), tritium ($\delta^{3}H$), and deuterium ($\delta^{2}H$) are excellent tracers for determining the origin of groundwater. $\delta^{2}H$, $\delta^{18}O$, and $\delta^{3}H$ analyses of spring waters from the Emirdağ basin field are presented in Table 1. The values for $\delta^{18}O$ and $\delta^{2}H$ of spring waters range from − 8.91 to − 11.56‰ and − 68.75 to − 74.32‰, respectively (Table 1). The origins and recharge conditions of waters were determined using the $\delta^{18}O$–$\delta^{2}H$ diagram. The relationship between the $\delta^{18}O$ and $\delta^{2}H$ values is plotted in Fig. 9. In this diagram, the following equations are defined:

- The global meteoric water line (GMWL) (Craig 1961)

$$\left(\delta^{2}H = 8\delta^{18}O + 10\right) \tag{3}$$

- The Ankara meteoric water line (AMWL) (IAEA/WMO 2004)

$$\left(\delta^{2}H = 8\delta^{18}O + 11.42\right) \tag{4}$$

The isotopic compositions of waters within the investigation area were compared with the GMWL and AMWL. The values plotted close to the GMWL were with d-excess value of 10% and the AMWL with d-excess value of 11.42‰. Water samples from the region were collected near the end of winter. The oxygen-18 and deuterium data from the Ağzıören spring in the study area suggest that there is evaporative enrichment of the stable isotopes (Fig. 3). The relation between oxygen-18 and deuterium values for the other spring sampling sites with the global meteoric water line and local meteoric water line (LMWL) shows that the samples fall above the GMWL and AMWL and close to winter precipitation. This indicates the winter precipitation (snow melt) as the predominant source of spring waters. If the aquifer has the same recharge area and mechanism or recharged with the same type of precipitation, the samples of this aquifer are located close to each other on the diagram. The samples collected in winter are more depleted in heavy isotopes. Low-surface temperatures inhibit isotope enrichment by the amount of effect during these months. The samples show the most negative values in the diagram (Fernández-Chacón et al. 2010).

Tritium in groundwater

Tritium is produced in the upper atmosphere. Relative residence time of groundwater was estimated based on the concentration of tritium (Clark and Fritz 1997). The $^{3}H < 1$ TU in waters indicates that they entered their present environment of residence before 1953 (Mazor 1991; Güleç and Mutlu 2002). The tritium concentrations in the spring water samples range from 0.96 to 5.04 TU (Table 1). The bivariate plot of $\delta^{18}O$ versus ^{3}H can be used for estimation of residence time of spring waters in the investigation area (Fig. 10). Waters having $^{3}H < 1$ TU have residence time older than 1953 (Clark and Fritz 1997), while values > 1 TU are regarded as submodern waters. According to Fig. 10, the Pınar spring sample shows values < 1 TU and the spring water has “old waters.” According to Fig. 10, other samples have values of > 1 TU and lie in the “submodern waters” field. Ravikumar and

Somashekar (2011) and Alçiçek et al. (2016) stated that tritium values varying from 1 to 8 TU are interpreted as an admixture of recent water with old groundwater and groundwater having been subjected to radioactive decay.

Tritium–chloride relationship is a method used for separating shallow and deep circulating waters (Çelmen and Çelik 2009; Bozdağ 2016). A plot of Cl^- versus ^3H in spring water samples is shown Fig. 11. The isotopic and geochemical analyses show that many of the spring waters consist predominantly of precipitation and springs generally are represented as shallow and have fast circulation. The Pınarbaşı spring has the lowest tritium (0.96 TU) value and shows deep and slow circulation and longer residence time (Fig. 11). The spring has an indication of surficial waters.

The deuterium excess

The origin of recharge of the groundwater is determined with the value of the deuterium excess (d-excess). Regionally, d-excess values vary due to differences in meteorological conditions. The d-excess values are defined by Eq. (5) (Dansgaard 1964):

$$\text{d}-\text{excess} = \delta^2\text{H}-8\delta^{18}\text{O} \qquad (5)$$

The d-excess values for the spring water samples in the investigation area ranged from 2.53 to 17.22‰, again reflecting inheritance from precipitation (Table 1). Higher d-excess was observed at Emirdede spring. Groundwater affected by evaporation represents higher value of $\delta^{18}O$ and lower d-excess values. So, during the process of evaporation, the residual water is enriched in heavier isotopes (Gupta and Deshpande 2005). Lower d-excess values (< 10‰) may be indicative of secondary evaporation of the locally formed clouds (Araguas-Araguas et al. 2000; Peng et al. 2007). Higher d-excess values (> 10‰) may possibly be due to the mixing of moisture sources (Mediterranean and local) (Jeelani et al. 2013).

Conclusions

The present study provides new data useful for assessing the quality and usability of springs in the Emirdağ basin. Emirdağ water springs in the region are utilized for drinking, irrigation, and domestic purposes. The springs are discharged from volcanic rocks and limestones. The spring waters are generally Ca^{2+} and HCO_3^- ion-rich waters. There was also a significant positive and strong correlation with Na^+, Ca^{2+}, Mg^{2+}, K^+, Cl^-, SO_4^{2-}, and HCO_3^- ions which indicates that they may be derived from rock–water interaction processes and ionic exchange. Calculations of chloroalkaline indices I and II show negative values. The negative values indicate the exchange of Mg^{2+} and Ca^{2+} in the water with Na^+ and K^+ in the rocks. According to the Gibbs diagram, all of the samples are on the field where “water–rock interaction” is active. According to the Schoeller diagram, all of the spring waters are in the class of “good quality–very good quality waters.” Generally, spring waters are suitable for irrigation criteria (EC, TDS, TH, Na%, SAR, SH, RSC, RSBC, PI, PS, SSP, MR, KR, K, and Ka) in the Emirdağ region except for the Pınarbaşı spring (EC = 790 μS/cm). According to the US Salinity Laboratory diagram, generally, spring waters are in the classes of C_1S_1, C_2S_1, and C_3S_1. Pınarbaşı spring water is of high salinity with low sodium water, so occasional soil washing measures should be taken to prevent salting and salt-sensitive plants should not be grown. In the Wilcox diagram, all spring waters are “very well-usable.” Usually, spring waters’ quality in the investigation area was affected by rock–water interaction and anthropogenic pollution. Nitrite and ammonium concentrations of waters were within the drinking water standard limits. The increase in nitrate in the results of the analysis is due to anthropogenic and agricultural pollution. The concentration of nitrate in the Ağzıören (64.09 mg/l) and Ufukpınar (62.01 mg/l) springs is exceeding the drinking water standard limit (50 mg/l) due to agricultural fertilization. Generally, trace element concentration values of spring waters do not exceed the limit values of the drinking water standards of WHO (2011) and TS-266 (2005). According to drinking water standards, the Al and As parameters surpass the threshold limits. The Al contents of Emirdağ spring (438 μg/l) and the As concentration (15.8 μ/l) at the Pınarbaşı spring exceed the drinking water standard limits due to water–rock interaction with volcanic rocks which have a wide spreading in the investigation area. The spring waters indicate a similarity in mechanism of recharge. The spring water samples are represented as shallow, have fast circulation, and are recharged. The Pınarbaşı spring has deep and slow circulation. The results of the study may help local governing bodies for the effective management of groundwater resources in the Emirdağ region.

References

Abdulhussein FM (2018) Hydrochemical assessment of groundwater of Dibdibba aquifer in Al-Zubair area, Basra, south of Iraq and its suitability for irrigation purposes. Iraqi, J Sci 59:135–143

Acarlar M, Güner E, Turhan N (2009) 1:100 000 ölçekli Türkiye Jeoloji Haritaları. No:118 Eskişehir-J26 paftası. MTA Genel Müdürlüğü Jeoloji Etütleri Dairesi Ankara

Ako AA, Shimada J, Hosono T, Kagabu M, Ayuk AR, Nkeng GE, Eyong GET, Takounjou ALF (2012) Spring water quality and usability in the Mount Cameroon area revealed by hydrogeochemistry. Environ Geochem Health 34(5):615–639

Alçiçek H, Bülbül A, Alçiçek MC (2016) Hydrogeochemistry of the thermal waters from the Yenice geothermal field (Denizli Basin, southwestern Anatolia, Turkey). J Volcanol Geotherm Res 309:118–138

APHA AWWA, WEF (2012) Standard Methods for examination of water and wastewater. 22nd ed. Washington: American Public Health Association 1360 pp

Araguas-Araguas L, Froehlich K, Rozanski K (2000) Deuterium and oxygen-18 isotope composition of precipitation and atmospheric moisture. Hydrol Process 14:1341–1355

Ardel A (1955) Yukarı Sakarya Havzası (Morfolojik Etüd). Türk Coğrafya Dergisi:1–24

Amano H, Nakagawa K, Berndtsson R (2018) Surface water chemistry and nitrate pollution in Shimabara, Nagasaki, Japan. Environ Earth Sci 77(9):354

Barbieri M, Nigro A, Petitta M (2017) Groundwater mixing in the discharge area of San Vittorino Plain (Central Italy): geochemical characterization and implication for drinking uses. Environ Earth Sci 76(11):393

Barbieri M, Ricolfi L, Vitale S, Muteto PV, Nigro A, Sappa G (2019) Assessment of groundwater quality in the buffer zone of Limpopo National Park, Gaza Province, Southern Mozambique. Environ Sci Pollut R 26(1):62–77

Bouchard DC, Williams MK, Surampalli RY (1992) Nitrate contamination of groundwater: sources and potential health effects. J Am Water Works Assoc 84(9):85–90

Bozdağ A (2016) Hydrogeochemical and isotopic characteristics of Kavak (Seydişehir-Konya) geothermal field, Turkey. J Afr Earth Sci 121:72–83

Canlı H (2007) Emirdağ havzası ve çevresinde doğal ortam ile insan arasındaki ilişkiler. Afyon Kocatepe Üniversitesi, Sosyal Bilimler Enstitüsü, Yüksek Lisans Tezi, 139 sayfa, (yayımlanmamış), Afyonkarahisar.

Catroll D (1962) Rain water as a chemical agent of geological process: a view USGS. Water Supply 1533:18–20

Comly HH (1945) Cyanosis in infants caused by nitrates in well water. J Am Med Assoc 129(2):112–116

Çelmen O, Çelik M (2009) Hydrochemistry and environmental isotope study of the geothermal water around Beypazarı granitoids, Ankara, Turkey. Environ Geol 58:689–1701

Clark ID, Fritz P (1997) Environmental isotopes in hydrogeology. Lewis, New York, p 328

Craig H (1961) Isotopic variations in meteoric waters. Science 133(3465):1702–1703

Dansgaard W (1964) Stable isotopes in precipitation. Tellus 16(4):436–468

Dehnavi AG, Sarikhani R, Nagaraju D (2011) Hydro geochemical and rock water interaction studies in east of Kurdistan, NW of Iran. Int J Environ Sci Res 1(1):16–22

Doneen LD (1962) The influence of crop and soil on percolating water pp156-163 In Proceedings of the Biennial Conference on Ground Water Recharge

DSİ (2018) http://bolge18.dsi.gov.tr/isletmedekitesisler/baraj-golet. Erişim tarihi ve saati: 26.04.2018, 06:16

Eaton FM (1950) Significance of carbonate in irrigation water. Soil Sci 69(2):123–133

Fedkiw J (1991) Nitrate occurrence in U.S. waters and related questions: a referenced summary of published sources from an agricultural perspective. Washington, District of Columbia: U.S. Department of Agriculture.

Fernández-Chacón F, Benavente J, Rubio-Campos JC, Kohfahl C, Jiménez J, Meyer H, Hubberten H, Pekdeger A (2010) Isotopic composition (δ^{18}O and δD) of precipitation and groundwater in a semi-arid, mountainous area (Guadiana Menor basin, Southeast Spain). Hydrol Process 24(10):1343–1356

Freeze RA, Cherry JA (1979) Groundwater Englewood Cliffs: Prentice-Hall

Erickson RL, Mosier EL, Odland SK, Erickson MS (1981) A favorable belt for possible mineral discovery in subsurface Cambrian rocks in southern Missouri. Economic Geology 76(4):921–933

Gibbs RJ (1970) Mechanism controlling world water chemistry. Science 170(3962):1088–1090

Güleç N, Mutlu H (2002) Isotope geochemistry in geothermal field. Summer School, Dokuz Eylül University, Application of earth science in geothermal, pp 74–103

Güler C, Thyne GD, McCray JE, Turner KA (2002) Evaluation of graphical and multivariate statistical methods for classification of water chemistry data. Hydrogeol J 10(4):455–474

Gupta IC (1983) Concept of residual sodium carbonate in irrigation waters in relation to sodic hazard in irrigated soils. Curr Agric 7(3/4):97–113

Gupta SK, Deshpande RD (2005) Groundwater isotopic investigations in India: what has been learned? Curr Sci 89(5):825–835

IAEA/WMO (2004) Global network of isotopes in precipitation. The GNIP Database

Iqbal HH, Shahid N, Qadir A, Ahmad SR, Sarwar S, Ashraf MR, Arshad HM, Masood N (2017) Hydrological and ichthyological impact assessment of Rasul Barrage, River Jhelum, Pakistan. Pol J Environ Stud 26

Jang CS, Chen CF, Liang CP, Chen JS (2016) Combining groundwater quality analysis and a numerical flow simulation for spatially establishing utilization strategies for groundwater and surface water in the Pingtung Plain. J Hydrol 533:541–556

Jeelani G, Kumar US, Kumar B (2013) Variation of δ18O and δD in precipitation and stream waters across the Kashmir Himalaya (India) to distinguish and estimate the seasonal sources of stream flow. J Hydrol 481:157–165

Kanduč T, Mori N, Kocman D, Stibilj V, Grassa F (2012) Hydrogeochemistry of Alpine springs from North Slovenia: insights from stable isotopes. Chem Geol 300:40–54

Kelley WP (1963) Use of saline irrigation water. Soil Sci 95(4):355–391

Khalid S (2019) An assessment of groundwater quality for irrigation and drinking purposes around brick kilns in three districts of Balochistan province, Pakistan, through water quality index and multivariate statistical approaches. J Geochem Explor 197:14–26

Kortatsi BK (2006) Hydrochemical characterization of groundwater in the Accra plains of Ghana. Environ Geol 50(3):299–311

Kumar PJS (2013) Interpretation of groundwater chemistry using piper and Chadha's diagrams: a comparative study from Perambalur Taluk. Elixir Geoscience 54:12208–12211

Larsen D, Swihart GH, Xiao Y (2001) Hydrochemistry and isotope composition of springs in the Tecopa basin, southeastern California, USA. Chem Geol 179(1-4):17–35

Li ZY, Yang N, Jing L, Yu P (2016) Major ion chemistry and quality assessment of groundwater in and around a mountainous tourist town of China. Expo Health 8:39–252

Maya AL, Loucks MD (1995) Solute and isotopic geochemistry and groundwater flow in the Central Wasatch Range, Utah. J Hydrol 172(1-4):31–59

Mazor E (1991) Applied chemical and isotopic groundwater hydrology, 1st edn. Open University Press, Buckingham, UK

Meriç BT, Çağırankaya S (2013) Sulak Alanlar. T.C. Orman ve Su İşleri Bakanlığı Doğa Koruma ve Milli Parklar Genel Müdürlüğü, Hassas Alanlar Dairesi Başkanlığı, Sulak Alanlar Şube Müdürlüğü, Kayıhan Ajans Turizm İnş. San. Tic. Ltd. Şti. Ankara, s:160

Michalik A (2008) The use of chemical and cluster analysis for studying spring water quality in Świętokrzyski National Park. Pol J Environ Stud 17(3):357–362

Mostaza-Colado D, Carreño-Conde F, Rasines-Ladero R, Iepure S (2018) Hydrogeochemical characterization of a shallow alluvial aquifer: 1 baseline for groundwater quality assessment and resource management. Sci Total Environ 639:1110–1125

Nayak KM, Sahood HK (2011) Assessment of ground-water quality in Tangi-Choudwar and Cuttack Blocks of Cuttack District, Orissa, India. Int J Earth Sci Eng 4(6):973–985

Nur A, Ishaku JM, Yusuf SN (2012) Groundwater flow patterns and hydrochemical facies distribution using geographical information system (GIS) in Damaturu, northeast Nigeria. Int J Geosci 3(05): 1096–1106

Omonona OV, Onwuka OS, Okogbue CO (2013) Characterization of groundwater quality in three settlement areas of Enugu metropolis, southeastern Nigeria, using multivariate analysis. Environ Monit Assess 186:651–664

Onwuka OS, Omonona OV (2017) Hydrogeochemical characteristics of coastal aquifers from Port Harcourt, southern Nigeria. Environ Earth Sci 76(17):609

Öcal H, Alan İ, Balcı V, Keskin H (2011) 1/100.000 ölçeklijeolojiharitası: Afyon-K26 paftası. Maden Tetkikve Arama Genel Müdürlüğü, Ankara

Özcan A, Göncüoğlu MC, Turhan N, Şentürk K, Uysal Ş, Işık A (1990) Konya-Kadınhan dolayının temel jeolojisi. MTA Rapor No:9535 (yayınlanmamış)

Peng H, Mayer B, Harris S, Krouse HR (2007) The influence of below-cloud secondary effects on the stable isotope composition of hydrogen and oxygen in precipitation at Calgary, Alberta, Canada. Tellus 59:698–704

Piper AM (1944) A graphic procedure in the geochemical interpretation of water analyses. EOS Trans Am Geophys Union 25(6):914–928

Prasad B, Bose J (2001) Evaluation of the heavy metal pollution index for surface and spring water near a limestone mining area of the lower Himalayas. Environ Geol 41(1-2):183–188

Raghunath HM (1987) Groundwater 2nd edn Wiley Eastern Ltd New Delhi 563p

Ragno G, De Luca M, Ioele G (2007) An application of cluster analysis and multivariate classification methods to spring water monitoring data. Microchem J 87(2):119–127

Rao NS (2008) Factors controlling the salinity in groundwater in parts of Guntur district, Andhra Pradesh, India. Environ Monit Assess 138(1-3):327–341

Ravikumar P, Somashekar RK (2011) Environmental Tritium (^{3}H) and hydrochemical investigations to evaluate groundwater in Varahi and Markandeya river basins, Karnataka, India. J Environ Radioact 102(2):153–162

Richards LA (1954) Diagnosis and improvement of saline alkali soils. US Department of Agriculture Handbook 60 pp. 160

Richards LA (1969) Diagnosis and improvement of saline and alkali soils. United States Department of Agricultura, Washington

Ryan M, Meiman J (1996) An examination of short-term variations in water quality at a karst spring in Kentucky. Groundwater 34(1):23–30

Saldivar A, Soto V (2009) Arsenic: an abundant natural poison. ProQuest Discovery Guides, http://www.csa.com/ discoveryguides/arsenic, Released March

Saleh A, Al-Ruwih F, Shehata M (1999) Hydrogeochemical process operating within the main aquifers of Kuwait. J Arid Environ 42:195–209

Sawyer GN, McMcartly DL (1967) Chemistry of sanitary engineers. 2nd edn McGraw Hill, New York 518p

Saxena V, Ahmed S (2001) Dissolution of fluoride in groundwater: a water-rock interaction study. Environ Geol 40(9):1084–1087

Schoeller H (1962) Les eaux souterraines. 642 p. Paris, France

Schoeller H (1965) Hydrodynamique lans lekarst (ecoulemented emmagusinement). Actes Colloques Doubronik, I, AIHS et UNESCO, pp. 3-20

Shigut DA, Liknew G, Irge DD, Ahmad T (2017) Assessment of physico-chemical quality of borehole and spring water sources supplied to Robe Town, Oromia region, Ethiopia. Appl Water Sci 7(1):155–164

Sousa MR, Rudolph DL, Frind EO (2014) Threats to groundwater resources in urbanizing watersheds: the Waterloo moraine and beyond. Can Water Resour J 39:2

Stallard RF, Edmond JM (1983) Geochemistry of the Amazon: 2. The influence of geology and weathering environment on the dissolved load. J Geophys Res Oceans 88(C14):9671–9688

Sun YB, Wang WK, Duan L (2014) Geochemical evolution mechanisms of shallow groundwater in Guanzhong Basin. Hydrogeology & Engineering Geology 41(3):29–35

Taheri M, Gharaie MHM, Mehrzad J, Afshari R, Datta S (2017) Hydrogeochemical and isotopic evaluation of arsenic contaminated waters in an argillic alteration zone. J Geochem Explor 175:1–10

Tahmasebi P, Mahmudy-Gharaie MH, Ghassemzadeh F, Karouyeh AK (2018) Assessment of groundwater suitability for irrigation in a gold mine surrounding area, NE Iran. Environ Earth Sci 77:766

Tiwari AK, De Maio M, Amanzio G (2017) Evaluation of metal contamination in the groundwater of the Aosta Valley Region, Italy. Int J Environ Res 11:291–300

TMMOB (2012) Karasukıyıalanıkıyıdaralmasıraporu, Türk Mühendis ve Mimar Odaları Birliği raporu, Mattek Basım Yayın Tanıtım Tic. San. Ltd. Şti, Ankara, 144 s

Todd DK (1960) Salt water intrusion of coastal aquifers in the United States. Internat Assoc Sci Hydrology (Gentbrugge Belgium) Pub52 p. 452-461

Todd DK (1980) Groundwater hydrology, 2nd edn. Wiley, New York, p 535

TS-266 (2005) İnsani tüketim amaçlı sular. Türk İçme Suyu Standartları TSE 266 sayılı standart-Türk Standartları Enstitüsü-Ankara

Türksoy VO (2010) Emirdağ kireçtaşlarının hammadde özelliklerinin incelenmesi. Afyon Kocatepe Üniversitesi, Fen Bilimleri Enstitüsü, Yüksek Lisans Tezi, Afyonkarahisar, 155 s

Umut M (2008) 1:100 000 ölçekli Türkiye Jeoloji Haritaları. No:92 Ilgın-K27 paftası, MTA Genel Müdürlüğü Jeoloji Etütleri Dairesi, Ankara

U.S. EPA (U.S. Environmental Protection Agency) (2012) Edition of the drinking water standards and health advisories. Washington, DC: U.S. EPA; 2012 [Available: https://water.epa.gov/action/advisories/drinking/upload/dwstandards2012.pdf Last accessed March 2013.]

Verma A, Shetty BK, Guddattu V, Chourasia MK, Pundir P (2017) High prevalence of dental fluorosis among adolescents is a growing concern: a school based cross-sectional study from Southern India. Environ Health Prev Med 22:17

Wagh VM, Panaskar DB, Jacobs JA, Mukate SV, Muley AA, Kadam AK (2019a) Influence of hydro-geochemical processes on groundwater quality through geostatistical techniques in Kadava river basin, western India. Arab J Geosci 12(1):7

Wagh VM, Panaskar DB, Mukate SV, Aamalawar ML, Laxman Sahu U (2019b) Nitrate associated health risks from groundwater of Kadava river basin, Nashik, Maharashtra, India. Hum Ecol Risk Assess Int J 1-19

WHO (2011) Guidelines for drinking-water quality, 4th edn. Organization, World Health

Wilcox LV (1955) Classification and use of irrigation water. USDA Circular, Washington DC, 969p

Wirtz D (1955) 73/1,2,3,4 Emirdağ ve Katrana paftalarında yapılan jeolojik harita çalışmaları hakkında rapor MTA Rap No: 2363, Ankara

Xu P, Feng W, Qian H, Zhang Q (2019) Hydrogeochemical characterization and irrigation quality assessment of shallow groundwater in the central-western Guanzhong Basin, China. Int J Environ Res Public Health 16(9):1492:1-18

Yakar M (2009) Emirdağ İlçesi Kırsalında Göçün Etkileri, Sorunları ve Çözüm Önerileri. Afyon Kocatepe Üniversitesi, Sosyal Bilimler Enstitüsü, Doktora Tezi, Afyonkarahisar, 310 s

Yıldız A, Bağcı M, Dumlupunar İ, Başaran C (2014) Afyonkarahisar İlinin Seramik Sektörü Hammadde Potansiyeli (025788) (553-564). Afyon Kocatepe Üniversitesi Fen ve Mühendislik Bilimleri Dergisi 14(3):553-564

Yılmaz F, Koltka S, Sabah E (2011) Emirdağ-Adaçal (Afyonkarahisar) Kireçtaşlarının Beton Agregaları Standardına Uygunluğunun Araştırılması (015801) (1-12). Afyon Kocatepe Üniversitesi Fen ve Mühendislik Bilimleri Dergisi 11(1):1-12

Yousef AF, Saleem AA, Baraka AM, Aglan OSH (2009) The impact of geological setting on the groundwater occurrences in some wadis in Shlatein-Abu Ramad area, SE Desert, Egypt. European Water 25(26):53–68